Alternative wavelets for the solution of variable-order fractal-fractional differential equations system with power and Mittag-Leffler kernels

Parisa Rahimkhani [a, *] **Salameh Sedaghat** [b]

[a] Faculty of Science, Mahallat Institute of Higher Education, Mahallat, Iran

[b] Department of Mathematics, Buein Zahra Technical University, Buein Zahra, Qazvin, Iran

Abstract

In this paper, a procedure based on the fractional-order alternative Legendre wavelets (FALWs) is introduced for solving variable-order fractal-fractional differential equations (VFFDEs) system with power and Mittag-Leffler kernels. An analytic formula is obtained for computing the variable-order fractal-fractional integral operator of the FALWs by employing the regularized beta functions. The presented method converts solving the primary problem to solving a system of nonlinear algebraic equations. To do this, the variable-order fractal-fractional (VFF) derivative of the unknown function is expanded in terms of the FALWs with unknown coefficients at first. Then, by employing the properties of the VFF derivative and integral, together with the collocation method, a system of algebraic equations is obtained, that can be easily solved by the Newton's iterative scheme. An error upper bound for the numerical solution in the Sobolev space is obtained. Finally, different chaotic oscillators of variable-order are solved in order to illustrate the accuracy and validity of the suggested strategy.

Keywords: Alternative Legendre wavelets, Variable-order fractal-fractional differential equations, Collocation method, Numerical method, Error estimate.
Mathematics Subject Classification (2010): 28A80, 65L60, 65T60.

1 Introduction

Fractional calculus is a hot topic of research that investigates various real-world problems, such as propagation of spherical flames [1], fluid mechanics [2], viscoelastic materials [3, 4], electromagnetism [5] economy [6], etc. Notice that the main reason for employing fractional operators in modeling various phenomena in engineering and physics is their ability to accurately describe processes with genetic and memory properties [7]. We remind that in recent years, various numerical techniques have been developed to solve fractional differential equations (FDEs), because analytical solutions of these problems are either impossible or only possible with unrealistic simplifications. Some of these algorithms are Müntz wavelets [8], Chelyshkov wavelets [9], fractional Chelyshkov wavelets [10], Taylor wavelets [11], fractional-order general Lagrange scaling functions [12], fractional-order Genocchi deep neural networks [13], Touchard-Ritz [14] algorithm etc.

In 2017, Atangana [15] introduced some new differential operators such as convolution of power, exponential and generalized Mittag-leffler functions with fractal derivative. These new definitions were called fractal-fractional differential operators. Indeed, a fractal-fractional operator is made up of the concepts of fractional differentiation (which have the non-local property) and fractal derivative (which have local property) in a single differentiation. In fact, the main purpose of fractal-fractional differentiation is to effectively represent fractal dynamics by substituting fractal time with continuous time. Similarly, if the system is fractal differentiable, then the fractal order derivative is proportional to $\beta t^{\beta-1}$. It is highly successful in the mathematical modeling of different areas of science, such as chaotic different problems [16], Ebola virus [17], drilling system [18], finance [19], Biology [20], etc. This fact prompts researchers to use numerical schemes to obtain approximate solutions for such problems. For instance, Müntz-Legendre polynomials scheme for

*Corresponding author: rahimkhani.parisa@gmail.com; rahimkhani.parisa@mahallat.ac.ir (P. Rahimkhani)

the numerical solution of fractal-fractional 2D optimal control problems (FFOCPs) [21], Legendre polynomials method for approximation of nonlinear FFOCPs [22], shifted Chebyshev cardinal functions for the numerical solution of coupled nonlinear fractal-fractional Schrödinger equations [23], shifted Vieta-Fibonacci polynomials method for solving fractal-fractional fifth-order KdV equation [24], spectral collocation method involving the shifted Legendre polynomials for solving fractal-fractional Kuramoto-Sivashinsky and Korteweg-de Vries equations [25], Lagrange polynomials method for solving fractal–fractional Michaelis–Menten enzymatic reaction model [26], generalized Lucas wavelet method for solving nonlinear fractal-fractional optimal control problems [27], and fractional shifted Morgan-Voyce neural networks for solving fractal-fractional pantograph differential equations [28].

A new type of fractal-fractional calculus gave birth to a new class of integral and differential equations such that there is not much work in the literature in this regard. The variable-order fractal- fractional calculus is defined as the extension of the constant-order fractal-fractional one. By this generalization, the order of fractional and dimensional of fractal are allowed to take any given function. Due to the memory property of such operators, they become a powerful tool for modeling complex systems in science and engineering [29]. Since these equations are highly complex, solving them analytically is difficult. Recently, few researchers have presented numerical schemes for solving VFFDEs. Aguilar et al. [30] applied artificial neural networks for solving fractal-fractional Mittag-Leffler differential equations of variable-order where the neural network is optimized by the Levenberg-Marquardt algorithm. Pérez and Aguilar [31] proposed a numerical method based on the Lagrangian piece-wise interpolation for delay VFFDEs with power, exponential and Mittag-Leffler laws.

In recent years, there has been an increasing interest in using wavelets for solving different classes of problems. The main reasons for such widespread applications are due to the fact that (i) after discretization, the coefficients matrix of algebraic equations is sparse. (ii) The solution is of multiresolution type. (iii) The wavelets scheme is computer oriented; so, solving higher-order equations becomes a matter of dimension increasing. (iv) The solution is convergent, even if the size of increment is large. In recent years, different classes of wavelets have been applied for the approximate solution of diverse problems. For instance, Bernoulli wavelets for fractional differential equations system [32], Hahn wavelets for fractional integro-differential equations [33], Legendre wavelets for fractional delay-type integro-differential equations [34], Bernstein wavelets for distributed-order fractional optimal control problems [35], and Taylor wavelets for initial and boundary value problems of the Bratu-type equations [36].

Since, there is a limited number of study related to the VFFDEs systems in the Caputo and Atangana-Riemann-Liouville sense, the following objectives in this paper are considered:

1. Defining a novel class of systems of variable-order fractal-fractional differential equations involved with derivatives in the Caputo and Atangana-Riemann-Liouville senses.

2. Introducing an exact formula for computing variable-order fractal-fractional integral operator (VFFIO) in terms of the regularized beta functions for the FALWs.

3. Presenting a feasibility and effectiveness strategy based on this operator and FALWs for the numerical solution of such problems.

So, we concentrate on the following class of VFFDEs system:

$$\begin{cases} {}_0\mathcal{D}_t^{\alpha(t),\beta(t)}\Xi_1(t) = \mathcal{F}_1(t,\Xi_1(t),\Xi_2(t),\ldots,\Xi_r(t)), \\ {}_0\mathcal{D}_t^{\alpha(t),\beta(t)}\Xi_2(t) = \mathcal{F}_2(t,\Xi_1(t),\Xi_2(t),\ldots,\Xi_r(t)), \\ \quad\vdots \qquad\qquad\qquad \vdots \\ {}_0\mathcal{D}_t^{\alpha(t),\beta(t)}\Xi_r(t) = \mathcal{F}_r(t,\Xi_1(t),\Xi_2(t),\ldots,\Xi_r(t)). \end{cases} \tag{1}$$

with the initial conditions

$$\Xi_i(0) = \wp_i, \qquad i = 1,2,\ldots,r, \tag{2}$$

where r is a given natural number, $\mathcal{F}_i$ for $i = 1,2,\ldots,r$ are continuous functions, ${}_0\mathcal{D}_t^{\alpha(t),\beta(t)}$ shows the variable-order fractal-fractional derivative of order $(\alpha(t),\beta(t))$ in the Caputo $({}_0^{CFF}\mathcal{D}_t^{\alpha(t),\beta(t)})$ or Atangana-Riemann-Liouville $({}_0^{ARLFF}\mathcal{D}_t^{\alpha(t),\beta(t)})$ sense, and $\wp_i$ for $i = 1,2,\ldots,r$ are given real constants.

In this work, we first construct an exact formula for the VFFIO of the FALWs by using the regularized beta function as

$$ {}_0^{CFF}\mathcal{I}_t^{\alpha(t),\beta(t)}\Psi^{(\theta)}(t) = \Upsilon(t,\alpha(t),\beta(t),\theta), \tag{3} $$

for the variable-order fractal-fractional integral (${}_0^{CFF}\mathcal{I}_t^{\alpha(t),\beta(t)}$) of order $(\alpha(t),\beta(t))$ in the Caputo sense, and

$$ {}_0^{ARLFF}\mathcal{I}_t^{\alpha(t),\beta(t)}\Psi^{(\theta)}(t) = \Lambda(t,\alpha(t),\beta(t),\theta), \tag{4} $$

for the variable-order fractal-fractional integral (${}_0^{ARLFF}\mathcal{I}_t^{\alpha(t),\beta(t)}$) of order $(\alpha(t),\beta(t))$ in the Atangana-Riemann-Liouville sense. Then, the functions ${}_0\mathcal{D}_t^{\alpha(t),\beta(t)}\Xi_i(t)$ for $i = 1,2,\ldots,r$ are approximated by the FALWs with unknown coefficients. By using these approximations, the VFF integral operators and the initial conditions, we approximate the functions $\Xi_i(t), i = 1,2,\ldots,r$. By substituting these approximations in the main problem, an algebraic system of nonlinear equations including unknown coefficients is obtained. Finally, this system is solved by the Newton's iterative method. The main advantages of the proposed method are:

- A small value of alternative Legendre wavelets is needed to achieve high accuracy and satisfactory results.
- By using this algorithm, considered problem is reduced into a system of algebraic equations that can be solved via a suitable numerical scheme.
- The obtained numerical solution with this method is a continuous and differentiable solution, also these solutions satisfy the initial conditions.
- This algorithm can be easily implemented to estimate the solution of VFFDEs defined on large intervals.
- There are two degrees of freedom (k, M) for wavelets but one degree of freedom (M) for polynomials.
- We obtain variable-order fractal-fractional integral operator of alternative Legendre wavelets without any error.

The rest of this paper is organized as follows: Section 2 recalls some useful definitions about fractal-fractional calculus and alternative wavelets. Section 3 introduces an exact formula for computing the VFFIO of the FALWs by applying the regularized beta function. Section 4 formulates the mentioned algorithm. An error upper bound for the numerical solution in the Sobolev space is obtained in Section 5. Section 6 presents three numerical examples to show the accuracy and efficiency of the proposed scheme. Finally, the main conclusions of the study are highlighted in Section 7.

2 Useful definitions

In this section, we recall some main definitions about fractal-fractional calculus and FALWs.

2.1 Fractal-fractional operators

In the continuation, we review some well-known fractal-fractional derivative and integral operators.

Definition 1. *The Mittag-Leffler function for one-parameter and two-parameter are defined as follows, respectively [37]*

$$ E_\vartheta(t) = \sum_{r=0}^{\infty} \frac{t^r}{\Gamma(r\vartheta+1)}, \qquad \vartheta \in R^+, t \in R, \tag{5} $$

and

$$ E_{\vartheta,\iota}(t) = \sum_{r=0}^{\infty} \frac{t^r}{\Gamma(r\vartheta+\iota)}, \qquad \vartheta,\iota \in R^+, t \in R. \tag{6} $$

Definition 2. *([31]) The Caputo variable-order fractal-fractional derivative of order* $(\alpha(t), \beta(t))$ *of the differential function* $\Xi(t)$ *is given by*

$$ {}_0^{CFF}D_t^{\alpha(t),\beta(t)}\Xi(t) = \frac{1}{\Gamma(1-\alpha(t))}\frac{d}{dt^{\beta(t)}}\int_0^t (t-s)^{-\alpha(t)}\Xi(s)ds, \tag{7} $$

where $0 < \alpha(t), \beta(t) \leq 1$.

Definition 3. *([31]) The Caputo variable-order fractal-fractional integral of order* $(\alpha(t), \beta(t))$ *of the continuous function* $\Xi(t)$ *is given by*

$$ {}_0^{CFF}\mathcal{I}_t^{\alpha(t),\beta(t)}\Xi(t) = \frac{\beta(t)}{\Gamma(\alpha(t))}\int_0^t (t-s)^{\alpha(t)-1}s^{\beta(t)-1}\Xi(s)ds. \tag{8} $$

Definition 4. *([31]) The Atangana-Riemann-Liouville variable-order fractal-fractional derivative of order* $(\alpha(t), \beta(t))$ *of the differential function* $\Xi(t)$ *is defined as*

$$ {}_0^{ARLFF}\mathcal{D}_t^{\alpha(t),\beta(t)}\Xi(t) = \frac{\mathcal{C}(\alpha(t))}{1-\alpha(t)}\frac{d}{dt^{\beta(t)}}\int_0^t E_{\alpha(t)}\left[\frac{-\alpha(t)(t-s)^{\alpha(t)}}{1-\alpha(t)}\right]\Xi(s)ds, \tag{9} $$

where $0 < \alpha(t), \beta(t) < 1, \mathcal{C}(\alpha(t)) = 1 - \alpha(t) + \frac{\alpha(t)}{\Gamma(\alpha(t))}$, *and* $E_{\alpha(t)}(t)$ *is the Mittag-Leffler function.*

Definition 5. *([31]) The Atangana-Riemann-Liouville variable-order fractal-fractional integral of order* $(\alpha(t), \beta(t))$ *of the continuous function* $\Xi(t)$ *is defined as*

$$ {}_0^{ARLFF}\mathcal{I}_t^{\alpha(t),\beta(t)}\Xi(t) = \frac{\alpha(t)\beta(t)}{\mathcal{C}(\alpha(t))}\int_0^t (t-s)^{\alpha(t)-1}s^{\beta(t)-1}\Xi(s)ds + \frac{\beta(t)(1-\alpha(t))t^{\beta(t)-1}}{\mathcal{C}(\alpha(t))}\Xi(t). \tag{10} $$

2.2 Fractional alternative Legendre wavelets

The FALWs are defined on $[0, h)$ as: [10]

$$ \psi_{n,m,\hat{m}}^{(\theta)}(t) = \begin{cases} \sqrt{(2m+1)\theta}2^{\frac{k-1}{2}}AL_{m,\hat{m}}^{(\theta)}\left(\frac{2^{k-1}}{h}t - \hat{n}\right), & \frac{\hat{n}}{2^{k-1}}h \leq t < \frac{\hat{n}+1}{2^{k-1}}h, \\ 0, & \text{otherwise}, \end{cases} \tag{11} $$

where $AL_{m,\hat{m}}^{(\theta)}(t)$ denotes the fractional-order alternative Legendre functions (FALFs) defined on $[0, 1)$.
The FALFs are defined by putting t^θ $(\theta > 0)$ instead of t in the alternative Legendre polynomials as [38]

$$ AL_{m,\hat{m}}^{(\theta)}(t) = \sum_{r=m}^{\hat{m}}(-1)^{r-m}\left(\begin{array}{c}\hat{m}-m\\ r-m\end{array}\right)\left(\begin{array}{c}\hat{m}+r+1\\ \hat{m}-m\end{array}\right)t^{r\theta}, \qquad m = 0, 1, \ldots, \hat{m}. \tag{12} $$

Theorem 1. *([38]) The FALFs are orthogonal with respect to the weight function* $\omega^{(\theta)}(t) = t^{(\theta-1)}$ *on* $[0, 1]$, *that is*

$$ \int_0^1 AL_{m,\hat{m}}^{(\theta)}(t)AL_{n,\hat{m}}^{(\theta)}(t)\omega(t)dt = \frac{\delta_{m,n}}{\theta(m+n+1)}. $$

Figure 1 shows the graphs of the FALWs with $\theta, t \in [0, 1]$ where $(k = 2, M = 10)$ and $(k = 3, M = 8)$.

3 Variable-order fractal-fractional integral operator of the FALWs

In this section, we calculate the variable-order fractal-fractional integral operator of FALWs in the Caputo and Atangana-Riemann-Liouville senses. For this aim, we first introduce the regularized beta function $I(t; a, b)$ for given real numbers a and b as [39]

$$ I(t; a, b) = \frac{\Gamma(a+b)}{\Gamma(a)\Gamma(b)}\int_0^t s^{a-1}(1-s)^{b-1}ds. \tag{13} $$

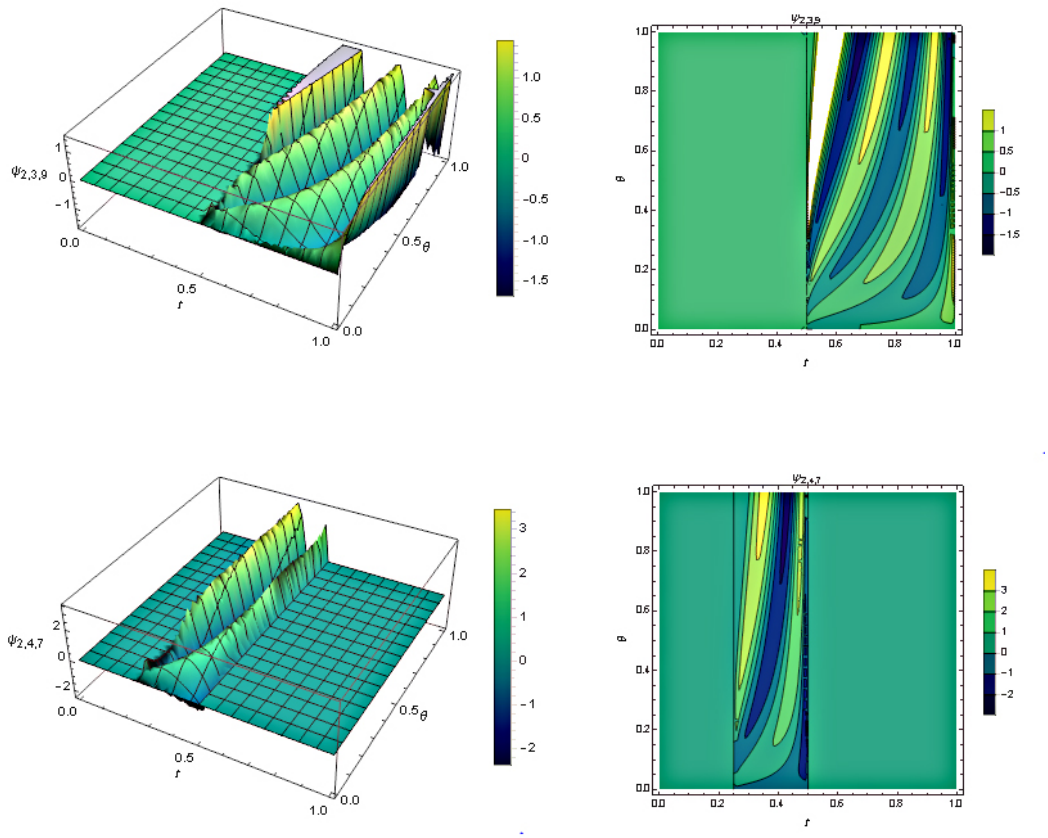

Figure 1: The graphs of the fractional-order alternative wavelets with $\theta, t \in [0,1]$ where $(k = 2, M = 10)$ (up) and $(k = 3, M = 8)$ (bottom).

3.1 Variable-order fractal-fractional integral operator with the CFF

Lemma 1. *The Caputo variable-order fractal-fractional integral of the function t^γ for $\gamma > 0$ is obtained as*

$$ {}_0^{CFF}\mathcal{I}_t^{\alpha(t),\beta(t)}(t^\gamma) = \frac{\beta(t)\Gamma(\beta(t)+\gamma)}{\Gamma(\alpha(t)+\beta(t)+\gamma)} t^{\alpha(t)+\beta(t)+\gamma-1}. \tag{14} $$

Proof. By using the definition of the Caputo fractal-fractional integral given in Eq. (8), we get

$$ \begin{aligned} {}_0^{CFF}\mathcal{I}_t^{\alpha(t),\beta(t)}(t^\gamma) &= \frac{\beta(t)}{\Gamma(\alpha(t))}\int_0^t s^{\beta(t)+\gamma-1}(t-s)^{\alpha(t)-1}ds \\ &= \frac{\beta(t)}{\Gamma(\alpha(t))}\int_0^t t^{\beta(t)+\gamma-1}\left(\frac{s}{t}\right)^{\beta(t)+\gamma-1} t^{\alpha(t)-1}\left(1-\frac{s}{t}\right)^{\alpha(t)-1} td\frac{s}{t}. \end{aligned} \tag{15} $$

By the change of variable $y = \frac{s}{t}$, and considering the definition of the regularized beta function (13), we have

$$ \begin{aligned} {}_0^{CFF}\mathcal{I}_t^{\alpha(t),\beta(t)}(t^\gamma) &= \frac{\beta(t)}{\Gamma(\alpha(t))} t^{\alpha(t)+\beta(t)+\gamma-1}\int_0^1 y^{\beta(t)+\gamma-1}(1-y)^{\alpha(t)-1}dy \\ &= \frac{\beta(t)\Gamma(\beta(t)+\gamma)}{\Gamma(\alpha(t)+\beta(t)+\gamma)} t^{\alpha(t)+\beta(t)+\gamma-1}. \end{aligned} \tag{16} $$

□

Theorem 2. *The Caputo variable-order fractal-fractional integral of the term $t^\gamma \mu_c(t)$ for $\gamma > 0$ is given by*

$$ {}_0^{CFF}\mathcal{I}_t^{\alpha(t),\beta(t)}(t^\gamma\mu_c(t)) = \frac{\beta(t)\Gamma(\beta(t)+\gamma)}{\Gamma(\alpha(t)+\beta(t)+\gamma)} t^{\alpha(t)+\beta(t)+\gamma-1}\left(1 - I\left(\frac{c}{t}, \beta(t)+\gamma, \alpha(t)\right)\right)\mu_c(t), \tag{17} $$

where μ_c is defined as

$$\mu_c(t) = \begin{cases} 1, & t \geq c, \\ 0, & otherwise. \end{cases}$$

Proof. We can conclude that the both sides of Eq. (17) are identically equal to zero over the interval $[0, c)$. Therefore, we can let $t \geq c$, then $\mu_c(t) = 1$. By using the definition of the Caputo variable-order fractal-fractional integral expressed in Eq. (8) for $t \geq c$, the following relation is achieved:

$$\begin{aligned}
{}_0^{CFF}\mathcal{I}_t^{\alpha(t),\beta(t)}(t^\gamma \mu_c(t)) &= \frac{\beta(t)}{\Gamma(\alpha(t))}\int_0^t (t-s)^{\alpha(t)-1} s^{\beta(t)-1} s^\gamma \mu_c(s) ds \\
&= \frac{\beta(t)}{\Gamma(\alpha(t))}\int_0^t (t-s)^{\alpha(t)-1} s^{\beta(t)+\gamma-1} ds - \frac{\beta(t)}{\Gamma(\alpha(t))}\int_0^c (t-s)^{\alpha(t)-1} s^{\beta(t)+\gamma-1} ds \\
&= {}_0^{CFF}\mathcal{I}_t^{\alpha(t),\beta(t)}(t^\gamma) - \frac{\beta(t)}{\Gamma(\alpha(t))}\int_0^c (t-s)^{\alpha(t)-1} s^{\beta(t)+\gamma-1} ds \\
&= {}_0^{CFF}\mathcal{I}_t^{\alpha(t),\beta(t)}(t^\gamma) - \frac{\beta(t)}{\Gamma(\alpha(t))}\int_0^c t^{\alpha(t)-1}\left(1-\frac{s}{t}\right)^{\alpha(t)-1} t^{\beta(t)+\gamma-1}\left(\frac{s}{t}\right)^{\beta(t)+\gamma-1} t d\frac{s}{t}.
\end{aligned} \tag{18}$$

Applying the change of variable $y = \frac{s}{t}$, and the regularized beta function (13), yield

$$\begin{aligned}
{}_0^{CFF}\mathcal{I}_t^{\alpha(t),\beta(t)}(t^\gamma \mu_c(t)) &= {}_0^{CFF}\mathcal{I}_t^{\alpha(t),\beta(t)}(t^\gamma) - \frac{\beta(t)}{\Gamma(\alpha(t))} t^{\alpha(t)+\beta(t)+\gamma-1}\int_0^{\frac{c}{t}} (1-y)^{\alpha(t)-1} y^{\beta(t)+\gamma-1} dy \\
&= {}_0^{CFF}\mathcal{I}_t^{\alpha(t),\beta(t)}(t^\gamma) - \frac{\beta(t)\Gamma(\beta(t)+\gamma)}{\Gamma(\alpha(t)+\beta(t)+\gamma)} t^{\alpha(t)+\beta(t)+\gamma-1} I\left(\frac{c}{t}, \beta(t)+\gamma, \alpha(t)\right) \\
&= \frac{\beta(t)\Gamma(\beta(t)+\gamma)}{\Gamma(\alpha(t)+\beta(t)+\gamma)} t^{\alpha(t)+\beta(t)+\gamma-1}\left(1 - I(\frac{c}{t}, \beta(t)+\gamma, \alpha(t))\right).
\end{aligned} \tag{19}$$

This completes the proof. □

Theorem 3. *The Caputo variable-order fractal-fractional integral operator of the vector $\Psi^\theta(t)$ can be given by*

$${}_0^{CFF}\mathcal{I}_t^{\alpha(t),\beta(t)}\Psi^{(\theta)}(t) = \Upsilon(t, \alpha(t), \beta(t), \theta), \tag{20}$$

where

$$\Psi^{(\theta)}(t) = [\psi_{1,0,M-1}^{(\theta)}(t), \psi_{1,1,M-1}^{(\theta)}(t), \dots \psi_{2^{k-1},M-1,M-1}^{(\theta)}(t)]^T, \tag{21}$$

$$\begin{aligned}
\Upsilon(t, \alpha(t), \beta(t), \theta) = \Big[&{}_0^{CFF}\mathcal{I}_t^{\alpha(t),\beta(t)}(\psi_{1,0,M-1}^{(\theta)}(t)), {}_0^{CFF}\mathcal{I}_t^{\alpha(t),\beta(t)}(\psi_{1,1,M-1}^{(\theta)}(t)), \dots \\
&{}_0^{CFF}\mathcal{I}_t^{\alpha(t),\beta(t)}(\psi_{2^{k-1},M-1,M-1}^{(\theta)}(t))\Big]^T.
\end{aligned}$$

Then, we have

$$
{}_{0}^{CFF}\mathcal{I}_{t}^{\alpha(t),\beta(t)}(\psi_{n,m,\hat{m}}^{(\theta)}(t)) = \begin{cases} 0, & 0 \leq t < \frac{\hat{n}}{2^{k-1}}h, \\ \sqrt{2^{k-1}(2m+1)\theta}\sum_{s=m}^{\hat{m}}\sum_{j=0}^{\lfloor \theta s \rfloor}(-1)^{s-m+\theta s-j}\begin{pmatrix} \hat{m}-m \\ s-m \end{pmatrix}\begin{pmatrix} \hat{m}+s+1 \\ \hat{m}-m \end{pmatrix} & \\ \begin{pmatrix} s\theta \\ j \end{pmatrix} 2^{(k-1)j}(\hat{n})^{\theta s-j}\frac{\beta(t)\Gamma(\beta(t)+j)}{h^{j}\Gamma(\alpha(t)+\beta(t)+j)}t^{\alpha(t)+\beta(t)+j-1}(1-I(\frac{\hat{n}}{2^{k-1}t}h,\beta(t)+j,\alpha(t))), & \\ \frac{\hat{n}}{2^{k-1}}h \leq t < \frac{\hat{n}+1}{2^{k-1}}h, & \\ \sqrt{2^{k-1}(2m+1)\theta}\sum_{s=m}^{\hat{m}}\sum_{j=0}^{\lfloor \theta s \rfloor}(-1)^{s-m+\theta s-j}\begin{pmatrix} \hat{m}-m \\ s-m \end{pmatrix}\begin{pmatrix} \hat{m}+s+1 \\ \hat{m}-m \end{pmatrix} & \\ \begin{pmatrix} s\theta \\ j \end{pmatrix} 2^{(k-1)j}(\hat{n})^{\theta s-j}\frac{\beta(t)\Gamma(\beta(t)+j)}{h^{j}\Gamma(\alpha(t)+\beta(t)+j)}t^{\alpha(t)+\beta(t)+j-1} & \\ (I(\frac{\hat{n}+1}{2^{k-1}t}h,\beta(t)+j,\alpha(t))-I(\frac{\hat{n}}{2^{k-1}t}h,\beta(t)+j,\alpha(t))), & \\ \frac{\hat{n}+1}{2^{k-1}}h \leq t < h. & \end{cases} \tag{22}
$$

Proof. We can rewrite the FALWs expressed in Eq. (11) as

$$
\psi_{n,m,\hat{m}}^{(\theta)}(t) = \sqrt{2^{k-1}(2m+1)\theta}\sum_{s=m}^{\hat{m}}(-1)^{s-m}\begin{pmatrix} \hat{m}-m \\ s-m \end{pmatrix}\begin{pmatrix} \hat{m}+s+1 \\ \hat{m}-m \end{pmatrix}(\frac{2^{k-1}t}{h}-\hat{n})^{s\theta}(\mu_{\frac{\hat{n}}{2^{k-1}}h}(t)-\mu_{\frac{\hat{n}+1}{2^{k-1}}h}(t)). \tag{23}
$$

According to the Binomial expansion, we obtain

$$
\begin{aligned}
\psi_{n,m,\hat{m}}^{(\theta)}(t) &= \sqrt{2^{k-1}(2m+1)\theta}\sum_{s=m}^{\hat{m}}\sum_{j=0}^{\lfloor s\theta \rfloor}(-1)^{s-m+s\theta-j}\begin{pmatrix} \hat{m}-m \\ s-m \end{pmatrix}\begin{pmatrix} \hat{m}+s+1 \\ \hat{m}-m \end{pmatrix}\begin{pmatrix} s\theta \\ j \end{pmatrix} \\
&\quad \frac{2^{(k-1)j}}{h^{j}}(\hat{n})^{s\theta-j}(t^{j}\mu_{\frac{\hat{n}}{2^{k-1}}h}(t)-t^{j}\mu_{\frac{\hat{n}+1}{2^{k-1}}h}(t)).
\end{aligned} \tag{24}
$$

Using the definition of the Caputo variable-order fractal-fractional integral introduced in Eq. (8) and Eq. (24), we have

$$
\begin{aligned}
{}_{0}^{CFF}\mathcal{I}_{t}^{\alpha(t),\beta(t)}(\psi_{n,m,\hat{m}}^{(\theta)}(t)) &= \sqrt{2^{k-1}(2m+1)\theta}\sum_{s=m}^{\hat{m}}\sum_{j=0}^{\lfloor s\theta \rfloor}(-1)^{s-m+s\theta-j}\begin{pmatrix} \hat{m}-m \\ s-m \end{pmatrix}\begin{pmatrix} \hat{m}+s+1 \\ \hat{m}-m \end{pmatrix}\begin{pmatrix} s\theta \\ j \end{pmatrix} \\
&\quad \frac{2^{(k-1)j}}{h^{j}}(\hat{n})^{s\theta-j}\Big({}_{0}^{CFF}\mathcal{I}_{t}^{\alpha(t),\beta(t)}(t^{j}\mu_{\frac{\hat{n}}{2^{k-1}}h}(t))-{}_{0}^{CFF}\mathcal{I}_{t}^{\alpha(t),\beta(t)}(t^{j}\mu_{\frac{\hat{n}+1}{2^{k-1}}h}(t))\Big) \\
&= \sqrt{2^{k-1}(2m+1)\theta}\sum_{s=m}^{\hat{m}}\sum_{j=0}^{\lfloor s\theta \rfloor}(-1)^{s-m+s\theta-j}\begin{pmatrix} \hat{m}-m \\ s-m \end{pmatrix}\begin{pmatrix} \hat{m}+s+1 \\ \hat{m}-m \end{pmatrix}\begin{pmatrix} s\theta \\ j \end{pmatrix} \\
&\quad \frac{2^{(k-1)j}}{h^{j}}(\hat{n})^{s\theta-j}\Big(\Big(\frac{\beta(t)\Gamma(\beta(t)+j)}{\Gamma(\alpha(t)+\beta(t)+j)}t^{\alpha(t)+\beta(t)+j-1}(1-I(\frac{\hat{n}}{2^{k-1}t}h,\beta(t)+j,\alpha(t)))\Big) \\
&\quad \mu_{\frac{\hat{n}}{2^{k-1}}h}(t)-\Big(\frac{\beta(t)\Gamma(\beta(t)+j)}{\Gamma(\alpha(t)+\beta(t)+j)}t^{\alpha(t)+\beta(t)+j-1} \\
&\quad (1-I(\frac{\hat{n}+1}{2^{k-1}t}h,\beta(t)+j,\alpha(t)))\Big)\mu_{\frac{\hat{n}+1}{2^{k-1}}h}(t)\Big),
\end{aligned} \tag{25}
$$

which completes the proof. □

Figures 2 and 3 show the graphs of the FALWs with $\alpha(t) = \tanh(t+5), \beta(t) = 0.99+\frac{0.01}{2}(\sin(t)+1), M = 8, h = 1$ where $k = 2$ and $k = 3$, respectively.

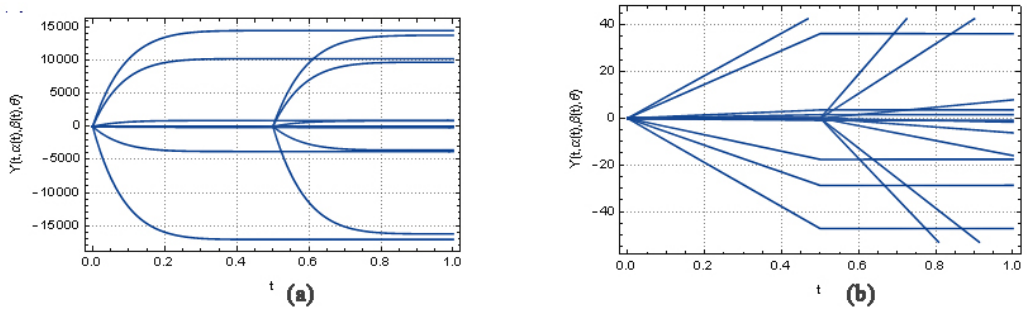

Figure 2: The graphs of the CFF variable-order integral with $k = 2, M = 8, h = 1, \alpha(t) = \tanh(t+5), \beta(t) = 0.99 + \frac{0.01}{2}(\sin(t)+1)$ where $(a) : \theta = 1$ and $(b) : \theta = \frac{1}{8}$.

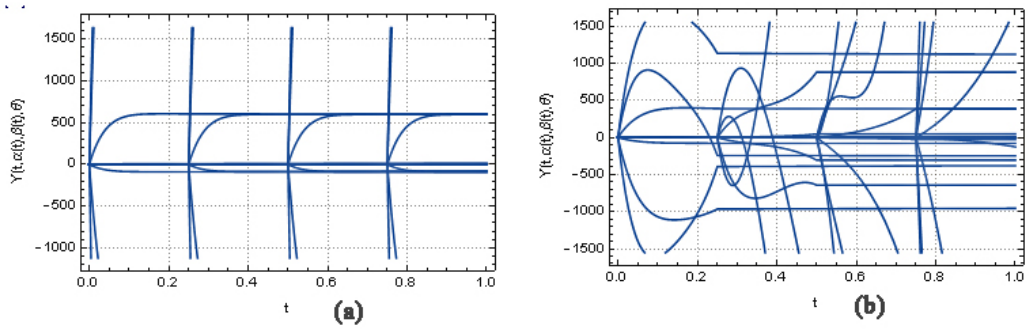

Figure 3: The graphs of the CFF variable-order integral with $k = 3, M = 8, h = 1, \alpha(t) = \tanh(t+5), \beta(t) = 0.99 + \frac{0.01}{2}(\sin(t)+1)$ where $(a) : \theta = 1$ and $(b) : \theta = \frac{2}{3}$.

3.2 Variable-order fractal-fractional integral with the ALRFF

Lemma 2. *The Atangana-Riemann-Liouville variable-order fractal-fractional integral of the term t^γ for $\gamma > 0$ is obtained as*

$$ {}_0^{ARLFF}\mathcal{I}_t^{\alpha(t),\beta(t)}(t^\gamma) = \frac{\alpha(t)\beta(t)\Gamma(\alpha(t))\Gamma(\beta(t)+\gamma)}{\mathcal{C}(\alpha(t))\Gamma(\alpha(t)+\beta(t)+\gamma)} t^{\alpha(t)+\beta(t)+\gamma-1} + \frac{\beta(t)(1-\alpha(t))}{\mathcal{C}(\alpha(t))} t^{\beta(t)+\gamma-1}. \quad (26) $$

Proof. With the help of the definition of the Atangana-Riemann-Liouville variable-order fractal-fractional integral expressed in Eq. (10), we have

$$ \begin{aligned} {}_0^{ARLFF}\mathcal{I}_t^{\alpha(t),\beta(t)}(t^\gamma) &= \frac{\alpha(t)\beta(t)}{\mathcal{C}(\alpha(t))} \int_0^t s^{\beta(t)+\gamma-1}(t-s)^{\alpha(t)-1} ds + \frac{\beta(t)(1-\alpha(t))}{\mathcal{C}(\alpha(t))} t^{\beta(t)+\gamma-1} \\ &= \frac{\alpha(t)\beta(t)}{\mathcal{C}(\alpha(t))} \int_0^t t^{\beta(t)+\gamma-1} (\frac{s}{t})^{\beta(t)+\gamma-1} t^{\alpha(t)-1} (1-\frac{s}{t})^{\alpha(t)-1} t d\frac{s}{t} \\ &+ \frac{\beta(t)(1-\alpha(t))}{\mathcal{C}(\alpha(t))} t^{\beta(t)+\gamma-1}. \end{aligned} \quad (27) $$

Using the change of variable $y = \frac{s}{t}$, and employing the regularized beta function (13), we get

$$ \begin{aligned} {}_0^{ARLFF}\mathcal{I}_t^{\alpha(t),\beta(t)}(t^\gamma) &= \frac{\alpha(t)\beta(t)}{\mathcal{C}(\alpha(t))} t^{\alpha(t)+\beta(t)+\gamma-1} \int_0^1 y^{\beta(t)+\gamma-1}(1-y)^{\alpha(t)-1} dy \\ &+ \frac{\beta(t)(1-\alpha(t))}{\mathcal{C}(\alpha(t))} t^{\beta(t)+\gamma-1} \\ &= \frac{\alpha(t)\beta(t)\Gamma(\alpha(t))\Gamma(\beta(t)+\gamma)}{\mathcal{C}(\alpha(t))\Gamma(\alpha(t)+\beta(t)+\gamma)} t^{\alpha(t)+\beta(t)+\gamma-1} + \frac{\beta(t)(1-\alpha(t))}{\mathcal{C}(\alpha(t))} t^{\beta(t)+\gamma-1}. \end{aligned} \quad (28) $$

□

Theorem 4. *The Atangana-Riemann-Liouville variable-order fractal-fractional integral of the term $t^\gamma \mu_c(t)$ for $\gamma > 0$ is obtained as*

$$\begin{aligned} {}_0^{ARLFF}\mathcal{I}_t^{\alpha(t),\beta(t)}(t^\gamma \mu_c(t)) &= \left(\frac{\alpha(t)\beta(t)\Gamma(\alpha(t))\Gamma(\beta(t)+\gamma)}{\mathcal{C}(\alpha(t))\Gamma(\alpha(t)+\beta(t)+\gamma)} t^{\alpha(t)+\beta(t)+\gamma-1}(1 - I(\frac{c}{t}, \beta(t)+\gamma, \alpha(t))) \right. \\ &+ \left. \frac{\beta(t)(1-\alpha(t))}{\mathcal{C}(\alpha(t))} t^{\beta(t)+\gamma-1}\right)\mu_c(t). \end{aligned} \tag{29}$$

Proof. Applying the definition of the Atangana-Riemann-Liouville variable-order fractal-fractional integral expressed in Eq. (10) for $t \geq c$, gives

$$\begin{aligned} {}_0^{ARLFF}\mathcal{I}_t^{\alpha(t),\beta(t)}(t^\gamma \mu_c(t)) &= \frac{\alpha(t)\beta(t)}{\mathcal{C}(\alpha(t))}\int_0^t (t-s)^{\alpha(t)-1} s^{\beta(t)-1} s^\gamma \mu_c(s) ds \\ &+ \frac{\beta(t)(1-\alpha(t))t^{\beta(t)+\gamma-1}\mu_c(t)}{\mathcal{C}(\alpha(t))} \\ &= \frac{\alpha(t)\beta(t)}{\mathcal{C}(\alpha(t))}\int_0^t (t-s)^{\alpha(t)-1} s^{\beta(t)+\gamma-1} ds \\ &- \frac{\alpha(t)\beta(t)}{\mathcal{C}(\alpha(t))}\int_0^c (t-s)^{\alpha(t)-1} s^{\beta(t)+\gamma-1} ds \\ &+ \frac{\beta(t)(1-\alpha(t))t^{\beta(t)+\gamma-1}}{\mathcal{C}(\alpha(t))} \\ &= {}_0^{ARLFF}\mathcal{I}_t^{\alpha(t),\beta(t)}(t^\gamma) - \frac{\alpha(t)\beta(t)}{\mathcal{C}(\alpha(t))}\int_0^c (t-s)^{\alpha(t)-1} s^{\beta(t)+\gamma-1} ds \\ &= {}_0^{ARLFF}\mathcal{I}_t^{\alpha(t),\beta(t)}(t^\gamma) \\ &- \frac{\alpha(t)\beta(t)}{\mathcal{C}(\alpha(t))}\int_0^c t^{\alpha(t)-1}(1-\frac{s}{t})^{\alpha(t)-1} t^{\beta(t)+\gamma-1}(\frac{s}{t})^{\beta(t)+\gamma-1} t d(\frac{s}{t}). \end{aligned} \tag{30}$$

By the change of variable $y = \frac{s}{t}$, and the regularized beta function (13), we have

$$\begin{aligned} {}_0^{ARLFF}\mathcal{I}_t^{\alpha(t),\beta(t)}(t^\gamma \mu_c(t)) &= {}_0^{ARLFF}\mathcal{I}_t^{\alpha(t),\beta(t)}(t^\gamma) \\ &- \frac{\alpha(t)\beta(t)}{\mathcal{C}(\alpha(t))} t^{\alpha(t)+\beta(t)+\gamma-1}\int_0^{\frac{c}{t}} (1-y)^{\alpha(t)-1} y^{\beta(t)+\gamma-1} dy \\ &= {}_0^{ARLFF}\mathcal{I}_t^{\alpha(t),\beta(t)}(t^\gamma) \\ &- \frac{\alpha(t)\beta(t)\Gamma(\beta(t)+\gamma)\Gamma(\alpha(t))}{\mathcal{C}(\alpha(t))\Gamma(\alpha(t)+\beta(t)+\gamma)} t^{\alpha(t)+\beta(t)+\gamma-1} I(\frac{c}{t}, \beta(t)+\gamma, \alpha(t)) \\ &= \frac{\alpha(t)\beta(t)\Gamma(\alpha(t))\Gamma(\beta(t)+\gamma)}{\mathcal{C}(\alpha(t))\Gamma(\alpha(t)+\beta(t)+\gamma)} t^{\alpha(t)+\beta(t)+\gamma-1} + \frac{\beta(t)(1-\alpha(t))}{\mathcal{C}(\alpha(t))} t^{\beta(t)+\gamma-1} \\ &- \frac{\alpha(t)\beta(t)\Gamma(\beta(t)+\gamma)\Gamma(\alpha(t))}{\mathcal{C}(\alpha(t))\Gamma(\alpha(t)+\beta(t)+\gamma)} t^{\alpha(t)+\beta(t)+\gamma-1} I(\frac{c}{t}, \beta(t)+\gamma, \alpha(t)) \\ &= \frac{\alpha(t)\beta(t)\Gamma(\beta(t)+\gamma)\Gamma(\alpha(t))}{\mathcal{C}(\alpha(t))\Gamma(\alpha(t)+\beta(t)+\gamma)} t^{\alpha(t)+\beta(t)+\gamma-1}(1 - I(\frac{c}{t}, \beta(t)+\gamma, \alpha(t))) \\ &+ \frac{\beta(t)(1-\alpha(t))}{\mathcal{C}(\alpha(t))} t^{\beta(t)+\gamma-1}. \end{aligned} \tag{31}$$

□

Theorem 5. *The Atangana-Riemann-Liouville variable-order fractal-fractional integral of the FALWs can be computed as*

$${}_0^{ARLFF}\mathcal{I}_t^{\alpha(t),\beta(t)}\Psi^{(\theta)}(t) = \Lambda(t, \alpha(t), \beta(t), \theta), \tag{32}$$

where

$$\Lambda(t,\alpha(t),\beta(t),\theta) = \Big[{}_0^{ARLFF}\mathcal{I}_t^{\alpha(t),\beta(t)}(\psi^{(\theta)}_{1,0,M-1}(t)), {}_0^{ARLFF}\mathcal{I}_t^{\alpha(t),\beta(t)}(\psi^{(\theta)}_{1,1,M-1}(t)),\dots \\ {}_0^{ARLFF}\mathcal{I}_t^{\alpha(t),\beta(t)}(\psi^{(\theta)}_{2^{k-1},M-1,M-1}(t))\Big]^T, \tag{33}$$

and

$${}_0^{ARLFF}\mathcal{I}_t^{\alpha(t),\beta(t)}(\psi^{(\theta)}_{n,m,\hat{m}}(t)) = \begin{cases} 0, & 0 \le t < \frac{\hat{n}}{2^{k-1}}h, \\ \sqrt{2^{k-1}(2m+1)\theta}\sum_{s=m}^{\hat{m}}\sum_{j=0}^{\lfloor\theta s\rfloor}(-1)^{s-m+\theta s-j}\begin{pmatrix}\hat{m}-m\\ s-m\end{pmatrix}\begin{pmatrix}\hat{m}+s+1\\ \hat{m}-m\end{pmatrix} \\ \begin{pmatrix}s\theta\\ j\end{pmatrix}2^{(k-1)j}(\hat{n})^{\theta s-j}\frac{\alpha(t)\beta(t)\Gamma(\alpha(t))\Gamma(\beta(t)+j)}{h^j\mathcal{C}(\alpha(t))\Gamma(\alpha(t)+\beta(t)+j)}t^{\alpha(t)+\beta(t)+j-1} \\ (1-I(\frac{\hat{n}}{2^{k-1}t}h,\beta(t)+j,\alpha(t)))+\frac{\beta(t)(1-\alpha(t))}{\mathcal{C}(\alpha(t))}t^{\beta(t)+j-1}, \\ \qquad\qquad \frac{\hat{n}}{2^{k-1}}h \le t < \frac{\hat{n}+1}{2^{k-1}}h, \\ \sqrt{2^{k-1}(2m+1)\theta}\sum_{s=m}^{\hat{m}}\sum_{j=0}^{\lfloor\theta s\rfloor}(-1)^{s-m+\theta s-j}\begin{pmatrix}\hat{m}-m\\ s-m\end{pmatrix}\begin{pmatrix}\hat{m}+s+1\\ \hat{m}-m\end{pmatrix} \\ \begin{pmatrix}s\theta\\ j\end{pmatrix}2^{(k-1)j}(\hat{n})^{\theta s-j}\frac{\alpha(t)\beta(t)\Gamma(\alpha(t))\Gamma(\beta(t)+j)}{h^j\mathcal{C}(\alpha(t))\Gamma(\alpha(t)+\beta(t)+j)}t^{\alpha(t)+\beta(t)+j-1} \\ (I(\frac{\hat{n}+1}{2^{k-1}t}h,\beta(t)+j,\alpha(t))-I(\frac{\hat{n}}{2^{k-1}t}h,\beta(t)+j,\alpha(t))), \\ \qquad\qquad \frac{\hat{n}+1}{2^{k-1}}h \le t < h. \end{cases} \tag{34}$$

Proof. Using the definition of the Atangana-Riemann-Liouville variable-order fractal-fractional integral provided in Eqs. (10) and (24), and Theorem 4, we obtain

$$\begin{aligned} {}_0^{ARLFF}\mathcal{I}_t^{\alpha(t),\beta(t)}(\psi^{(\theta)}_{n,m,\hat{m}}(t)) &= \sqrt{2^{k-1}(2m+1)\theta}\sum_{s=m}^{\hat{m}}\sum_{j=0}^{\lfloor\theta s\rfloor}(-1)^{s-m+\theta s-j}\begin{pmatrix}\hat{m}-m\\ s-m\end{pmatrix}\begin{pmatrix}\hat{m}+s+1\\ \hat{m}-m\end{pmatrix}\begin{pmatrix}s\theta\\ j\end{pmatrix} \\ &\quad \frac{2^{(k-1)j}}{h^j}(\hat{n})^{\theta s-j}\Big({}_0^{ARLFF}\mathcal{I}_t^{\alpha(t),\beta(t)}(t^j\mu_{\frac{\hat{n}}{2^{k-1}}h}(t)) - {}_0^{ARLFF}\mathcal{I}_t^{\alpha(t),\beta(t)}(t^j\mu_{\frac{\hat{n}+1}{2^{k-1}}h}(t))\Big) \\ &= \sqrt{2^{k-1}(2m+1)\theta}\sum_{s=m}^{\hat{m}}\sum_{j=0}^{\lfloor\theta s\rfloor}(-1)^{s-m+\theta s-j}\begin{pmatrix}\hat{m}-m\\ s-m\end{pmatrix}\begin{pmatrix}\hat{m}+s+1\\ \hat{m}-m\end{pmatrix}\begin{pmatrix}s\theta\\ j\end{pmatrix} \\ &\quad \frac{2^{(k-1)j}}{h^j}(\hat{n})^{\theta s-j}\Big(\Big(\frac{\alpha(t)\beta(t)\Gamma(\beta(t)+j)\Gamma(\alpha(t))}{\mathcal{C}(\alpha(t))\Gamma(\alpha(t)+\beta(t)+j)}t^{\alpha(t)+\beta(t)+j-1} \\ &\quad (1-I(\frac{\hat{n}}{2^{k-1}t}h,\beta(t)+j,\alpha(t)))+\frac{\beta(t)(1-\alpha(t))}{\mathcal{C}(\alpha(t))}t^{\beta(t)+j-1}\Big)\mu_{\frac{\hat{n}}{2^{k-1}}h}(t) \\ &- \Big(\frac{\alpha(t)\beta(t)\Gamma(\beta(t)+j)\Gamma(\alpha(t))}{\mathcal{C}(\alpha(t))\Gamma(\alpha(t)+\beta(t)+j)}t^{\alpha(t)+\beta(t)+j-1}(1-I(\frac{\hat{n}+1}{2^{k-1}t},\beta(t)+j,\alpha(t))) \\ &+ \frac{\beta(t)(1-\alpha(t))}{\mathcal{C}(\alpha(t))}t^{\beta(t)+j-1}\Big)\mu_{\frac{\hat{n}+1}{2^{k-1}}h}(t)\Big). \end{aligned} \tag{35}$$

□

So, the Theorem is proved.

4 Method of the solution

In this study, we consider the following two classes of systems of VFFDEs:
Problem (a):

$$\begin{cases} {}_0^{CFF}D_t^{\alpha(t),\beta(t)}\Xi_1(t) = \mathcal{F}_1(t,\Xi_1(t),\Xi_2(t),\ldots,\Xi_r(t)), \\ {}_0^{CFF}D_t^{\alpha(t),\beta(t)}\Xi_2(t) = \mathcal{F}_2(t,\Xi_1(t),\Xi_2(t),\ldots,\Xi_r(t)), \\ \quad\vdots \qquad\qquad\qquad \vdots \\ {}_0^{CFF}D_t^{\alpha(t),\beta(t)}\Xi_r(t) = \mathcal{F}_r(t,\Xi_1(t),\Xi_2(t),\ldots,\Xi_r(t)). \end{cases} \tag{36}$$

Problem (b):

$$\begin{cases} {}_0^{ARLFF}D_t^{\alpha(t),\beta(t)}\Xi_1(t) = \mathcal{F}_1(t,\Xi_1(t),\Xi_2(t),\ldots,\Xi_r(t)), \\ {}_0^{ARLFF}D_t^{\alpha(t),\beta(t)}\Xi_2(t) = \mathcal{F}_2(t,\Xi_1(t),\Xi_2(t),\ldots,\Xi_r(t)), \\ \quad\vdots \qquad\qquad\qquad \vdots \\ {}_0^{ARLFF}D_t^{\alpha(t),\beta(t)}\Xi_r(t) = \mathcal{F}_r(t,\Xi_1(t),\Xi_2(t),\ldots,\Xi_r(t)), \end{cases} \tag{37}$$

with the initial conditions

$$\Xi_i(0) = \wp_i, \qquad i = 1,2,\ldots,r. \tag{38}$$

In the sequence, we introduce a numerical strategy for solving the problems (a) and (b). For this aim, we apply the following steps:

Step 1. We approximate the fractal-fractional terms ${}_0\mathcal{D}_t^{\alpha(t),\beta(t)}\Xi_i(t), i = 1,2,\ldots,r$ by the FALWs as

$$\begin{aligned} {}_0^{CFF}D_t^{\alpha(t),\beta(t)}\Xi_1(t) &\simeq \sum_{n=1}^{2^{k-1}}\sum_{m=0}^{M-1} c_{n,m}^{(1)}\psi_{n,m,\hat{m}}^{(\theta)}(t) = C_1^T\Psi^{(\theta)}(t), \\ {}_0^{CFF}D_t^{\alpha(t),\beta(t)}\Xi_2(t) &\simeq \sum_{n=1}^{2^{k-1}}\sum_{m=0}^{M-1} c_{n,m}^{(2)}\psi_{n,m,\hat{m}}^{(\theta)}(t) = C_2^T\Psi^{(\theta)}(t), \\ &\vdots \qquad\qquad\qquad \vdots \\ {}_0^{CFF}D_t^{\alpha(t),\beta(t)}\Xi_r(t) &\simeq \sum_{n=1}^{2^{k-1}}\sum_{m=0}^{M-1} c_{n,m}^{(r)}\psi_{n,m,\hat{m}}^{(\theta)}(t) = C_r^T\Psi^{(\theta)}(t). \end{aligned} \tag{39}$$

Step 2. With the help of the variable-order fractal-fractional integral operator (20) and relation (39), along with the expressed initial conditions, we can approximate the unknown functions $\Xi_i(t), i = 1,2,\ldots,r$ as

$$\begin{aligned} \Xi_1(t) &\simeq \Upsilon(t,\alpha(t),\beta(t),\theta) + \wp_1, \\ \Xi_2(t) &\simeq \Upsilon(t,\alpha(t),\beta(t),\theta) + \wp_2, \\ &\vdots \qquad\qquad\qquad \vdots \\ \Xi_r(t) &\simeq \Upsilon(t,\alpha(t),\beta(t),\theta) + \wp_r. \end{aligned} \tag{40}$$

Step 3. By substituting the approximations (39)-(40) into relation (36), we get

$$\begin{cases} C_1^T\Psi^{(\theta)}(t) = \mathcal{F}_1(t,\Upsilon(t,\alpha(t),\beta(t),\theta)+\wp_1,\Upsilon(t,\alpha(t),\beta(t),\theta)+\wp_2,\ldots,\Upsilon(t,\alpha(t),\beta(t),\theta)+\wp_r), \\ C_2^T\Psi^{(\theta)}(t) = \mathcal{F}_2(t,\Upsilon(t,\alpha(t),\beta(t),\theta)+\wp_1,\Upsilon(t,\alpha(t),\beta(t),\theta)+\wp_2,\ldots,\Upsilon(t,\alpha(t),\beta(t),\theta)+\wp_r), \\ \quad\vdots \qquad\qquad\qquad \vdots \\ C_r^T\Psi^{(\theta)}(t) = \mathcal{F}_r(t,\Upsilon(t,\alpha(t),\beta(t),\theta)+\wp_1,\Upsilon(t,\alpha(t),\beta(t),\theta)+\wp_2,\ldots,\Upsilon(t,\alpha(t),\beta(t),\theta)+\wp_r). \end{cases} \tag{41}$$

Step 4. We define the residual functions $\mathcal{R}_i(t), i = 1,2,\ldots,r$ as

$$\begin{cases} \mathcal{R}_1(t) = C_1^T\Psi^{(\theta)}(t) - \mathcal{F}_1(t,\Upsilon(t,\alpha(t),\beta(t),\theta)+\wp_1,\Upsilon(t,\alpha(t),\beta(t),\theta)+\wp_2,\ldots,\Upsilon(t,\alpha(t),\beta(t),\theta)+\wp_r), \\ \mathcal{R}_2(t) = C_2^T\Psi^{(\theta)}(t) - \mathcal{F}_2(t,\Upsilon(t,\alpha(t),\beta(t),\theta)+\wp_1,\Upsilon(t,\alpha(t),\beta(t),\theta)+\wp_2,\ldots,\Upsilon(t,\alpha(t),\beta(t),\theta)+\wp_r), \\ \quad\vdots \qquad\qquad\qquad\qquad \vdots \\ \mathcal{R}_r(t) = C_r^T\Psi^{(\theta)}(t) - \mathcal{F}_r(t,\Upsilon(t,\alpha(t),\beta(t),\theta)+\wp_1,\Upsilon(t,\alpha(t),\beta(t),\theta)+\wp_2,\ldots,\Upsilon(t,\alpha(t),\beta(t),\theta)+\wp_r). \end{cases} \tag{42}$$

Step 5. By collocating the system (42) at the zeros of the shifted Legendre polynomials, we achieve

$$\begin{cases} \mathcal{R}_1(t_\iota) = 0, \\ \mathcal{R}_2(t_\iota) = 0, \\ \quad \vdots \\ \mathcal{R}_r(t_\iota) = 0, \end{cases} \tag{43}$$

where $\iota = 1, 2, \ldots, 2^{k-1}M$. So, we achieve a system of $r2^{k-1}M$ nonlinear algebraic equations with $r2^{k-1}M$ unknown coefficients, which can be solved via the Newton's iterative method.

Remark 1. *The problem (b) can be solved similar to the problem (a).*

5 Error bound

In this section, we achieve an error upper bound for the numerical solution in Sobolev space. The Sobolev norm of integer order $\tau \geq 0$ in the interval (a, b), can be expressed as follows: [40]

$$\|\Xi\|_{H^\tau(a,b)} = \left(\sum_{j=0}^{\tau} \int_a^b |\Xi^{(j)}(t)| dt \right)^{\frac{1}{2}} = \left(\sum_{j=0}^{\tau} \|\Xi^{(j)}(t)\|^2_{L^2(a,b)} \right)^{\frac{1}{2}}, \tag{44}$$

where $\Xi^{(j)}$ represents the distributional derivative of Ξ of order j.

Theorem 6. *([41]) Assume that $\Xi \in H^\tau(0,1)$ where $\tau \geq 0$ and $M \geq \tau$, and $\Xi^\star$ is the best approximation of Ξ which is approximated using the FALWs, then we have*

$$\|\Xi - \Xi^\star\|_{L^2(0,1)} \leq c(M-1)^{-\tau}(2^{k-1})^{-\tau}\|\Xi^{(\tau)}\|_{L^2(0,1)}, \tag{45}$$

and for $1 \leq s \leq \tau$, we have

$$\|\Xi - \Xi^\star\|_{H^s(0,1)} \leq c(M-1)^{2s-\frac{1}{2}-\tau}(2^{k-1})^{s-\tau}\|\Xi^{(\tau)}\|_{L^2(0,1)}. \tag{46}$$

Theorem 7. *If the hypothesizes in the Theorem 6 are valid, and $\mathcal{F}_i, i = 1, 2, \ldots, r$ satisfy the Lipshitz condition with constants $\eta_i, i = 1, 2, \ldots, r$, then we get*

$$\begin{aligned} \|Total\ Error\|_{L^2(\Omega)} \quad \leq \quad & \max_{1\leq i\leq r} \left(\max_{t\in\Omega} \left| \frac{\beta(t)\eta_i}{\Gamma(\alpha(t))} \sqrt{\frac{r\Gamma(2\alpha(t)-1)\Gamma(2\beta(t)-1)}{\Gamma(2\alpha(t)+2\beta(t)-2)}} t^{\alpha(t)+\beta(t)-\frac{3}{2}} \right| \right. \\ & \left. \left(\eta_i\sqrt{r} \left(\sum_{j=1}^{r} c^2(M-1)^{-2\tau}(2^{k-1})^{-2\tau}\|\Xi_j^{(\tau)}\|^2_{L^2(\Omega)} \right)^{\frac{1}{2}} + \|\mathcal{R}_i(t)\|_{L^2(\Omega)} \right) \right), \end{aligned} \tag{47}$$

where

$$\|Total\ Error\|_{L^2(\Omega)}\| = \|\Xi - \Xi^\star\|_{L^2(\Omega)}, \qquad \Omega = (0,1).$$

Proof. According to Eqs. (36) and (42), for the exact solution $\Xi(t)$ and the approximate solution $\Xi^\star(t)$, we have

$${}_0^{CFF}\mathcal{D}_t^{\alpha(t),\beta(t)}\Xi_i(t) = \mathcal{F}_i(t, \Xi_1(t), \Xi_2(t), \ldots, \Xi_r(t)), \quad i = 1, 2, \ldots, r, \tag{48}$$

and

$${}_0^{CFF}\mathcal{D}_t^{\alpha(t),\beta(t)}\Xi_i^\star(t) = \mathcal{F}_i(t, \Xi_1^\star(t), \Xi_2^\star(t), \ldots, \Xi_r^\star(t)) + \mathcal{R}_i(t), \quad i = 1, 2, \ldots, r. \tag{49}$$

By subtracting Eq. (49) from Eq. (48) and taking the variable-order fractal-fractional integral on both sides of the relation, we get

$$\begin{aligned} \Xi_i(t) - \Xi_i^\star(t) \quad = \quad & {}_0^{CFF}\mathcal{I}_t^{\alpha(t),\beta(t)}(\mathcal{F}_i(t, \Xi_1(t), \Xi_2(t), \ldots, \Xi_r(t)) \\ - \quad & \mathcal{F}_i(t, \Xi_1^\star(t), \Xi_2^\star(t), \ldots, \Xi_r^\star(t))) - {}_0^{CFF}\mathcal{I}_t^{\alpha(t),\beta(t)}(\mathcal{R}_i(t)). \end{aligned} \tag{50}$$

Employing the definition of the Caputo variable-order fractal-fractional integral (8) and the Schwarz's inequality, we deduce

$$\begin{aligned}
&\left|{}_0^{CFF}\mathcal{I}_t^{\alpha(t),\beta(t)}(\mathcal{F}_i(t,\Xi_1(t),\Xi_2(t),\ldots,\Xi_r(t))-\mathcal{F}_i(t,\Xi_1^\star(t),\Xi_2^\star(t),\ldots,\Xi_r^\star(t)))\right|\\
=&\left|\frac{\beta(t)}{\Gamma(\alpha(t))}\int_0^t(t-s)^{\alpha(t)-1}s^{\beta(t)-1}(\mathcal{F}_i(s,\Xi_1(s),\Xi_2(s),\ldots,\Xi_r(s))-\mathcal{F}_i(s,\Xi_1^\star(s),\Xi_2^\star(s),\ldots,\Xi_r^\star(s)))ds\right|\\
\leq&\frac{\beta(t)}{\Gamma(\alpha(t))}\bigg(\int_0^t(t-s)^{2\alpha(t)-2}s^{2\beta(t)-2}ds\bigg)^{\frac{1}{2}}\\
\times&\left(\int_0^t(\mathcal{F}_i(s,\Xi_1(s),\Xi_2(s),\ldots,\Xi_r(s))-\mathcal{F}_i(s,\Xi_1^\star(s),\Xi_2^\star(s),\ldots,\Xi_r^\star(s)))^2ds\right)^{\frac{1}{2}}.
\end{aligned}\tag{51}$$

From the definition of the regularized beta function (13), we have

$$\int_0^t(t-s)^{2\alpha(t)-2}s^{2\beta(t)-2}ds=\frac{\Gamma(2\alpha(t)-1)\Gamma(2\beta(t)-1)}{\Gamma(2\alpha(t)+2\beta(t)-2)}t^{2\alpha(t)+2\beta(t)-3}.\tag{52}$$

By considering the Lipshitz condition of the functions $\mathcal{F}_i$, and the relation $(\sum_{i=1}^n x_i)^2\leq n\sum_{i=1}^n x_i^2$, we get

$$\begin{aligned}
&\int_0^t(\mathcal{F}_i(s,\Xi_1(s),\Xi_2(s),\ldots,\Xi_r(s))-\mathcal{F}_i(s,\Xi_1^\star(s),\Xi_2^\star(s),\ldots,\Xi_r^\star(s)))^2ds\\
\leq&\int_0^t\bigg(\eta_i|\Xi_1(s)-\Xi_1^\star(s)|+\eta_i|\Xi_2(s)-\Xi_2^\star(s)|+\ldots+\eta_i|\Xi_r(s)-\Xi_r^\star(s)|\bigg)^2ds\\
\leq&\int_0^t\eta_i^2r\sum_{j=1}^r|\Xi_j(s)-\Xi_j^\star(s)|^2ds\leq\eta_i^2r\sum_{j=1}^r\int_0^1|\Xi_j(s)-\Xi_j^\star(s)|^2ds\\
\leq&\eta_i^2r\sum_{j=1}^r\|\Xi_j-\Xi_j^\star\|^2_{L^2(\Omega)}.
\end{aligned}\tag{53}$$

From Eqs. (51)-(53), we obtain

$$\begin{aligned}
&\left|{}_0^{CFF}\mathcal{I}_t^{\alpha(t),\beta(t)}(\mathcal{F}_i(t,\Xi_1(t),\Xi_2(t),\ldots,\Xi_r(t))-\mathcal{F}_i(t,\Xi_1^\star(t),\Xi_2^\star(t),\ldots,\Xi_r^\star(t)))\right|\\
\leq&\frac{\beta(t)\eta_i}{\Gamma(\alpha(t))}\sqrt{\frac{r\Gamma(2\alpha(t)-1)\Gamma(2\beta(t)-1)}{\Gamma(2\alpha(t)+2\beta(t)-2)}}t^{\alpha(t)+\beta(t)-\frac{3}{2}}\bigg(\sum_{j=1}^r\|\Xi_j-\Xi_j^\star\|^2_{L^2(\Omega)}\bigg)^{\frac{1}{2}}\\
\leq&max_{t\in\Omega}\left|\frac{\beta(t)\eta_i}{\Gamma(\alpha(t))}\sqrt{\frac{r\Gamma(2\alpha(t)-1)\Gamma(2\beta(t)-1)}{\Gamma(2\alpha(t)+2\beta(t)-2)}}t^{\alpha(t)+\beta(t)-\frac{3}{2}}\right|\bigg(\sum_{j=1}^r\|\Xi_j-\Xi_j^\star\|^2_{L^2(\Omega)}\bigg)^{\frac{1}{2}}.
\end{aligned}\tag{54}$$

Also, for $\left|{}_0^{CFF}\mathcal{I}_t^{\alpha(t),\beta(t)}\mathcal{R}_i(t)\right|$, we get

$$\begin{aligned}
\left|{}_0^{CFF}\mathcal{I}_t^{\alpha(t),\beta(t)}\mathcal{R}_i(t)\right|&=\left|\frac{\beta(t)}{\Gamma(\alpha(t))}\int_0^t(t-s)^{\alpha(t)-1}s^{\beta(t)-1}\mathcal{R}_i(s)ds\right|\\
&\leq\max_{t\in\Omega}\left|\frac{\beta(t)}{\Gamma(\alpha(t))}\sqrt{\frac{\Gamma(2\alpha(t)-1)\Gamma(2\beta(t)-1)}{\Gamma(2\alpha(t)+2\beta(t)-2)}}t^{\alpha(t)+\beta(t)-\frac{3}{2}}\right|\|\mathcal{R}_i\|_{L^2(\Omega)}.
\end{aligned}\tag{55}$$

From Eqs. (50), (52) and (55), we achieve

$$\begin{aligned}
\|\Xi_i-\Xi_i^\star\|_{L^2(\Omega)}\leq&\max_{t\in\Omega}\left|\frac{\beta(t)\eta_i}{\Gamma(\alpha(t))}\sqrt{\frac{r\Gamma(2\alpha(t)-1)\Gamma(2\beta(t)-1)}{\Gamma(2\alpha(t)+2\beta(t)-2)}}t^{\alpha(t)+\beta(t)-\frac{3}{2}}\right|\bigg(\sum_{j=1}^r\|\Xi_j-\Xi_j^\star\|^2_{L^2(\Omega)}\bigg)^{\frac{1}{2}}\\
+&\max_{t\in\Omega}\left|\frac{\beta(t)}{\Gamma(\alpha(t))}\sqrt{\frac{\Gamma(2\alpha(t)-1)\Gamma(2\beta(t)-1)}{\Gamma(2\alpha(t)+2\beta(t)-2)}}t^{\alpha(t)+\beta(t)-\frac{3}{2}}\right|\|\mathcal{R}_i\|_{L^2(\Omega)}.
\end{aligned}\tag{56}$$

By applying Eq. (45) and (56) for $i = 1, 2, \ldots, r$, we obtain

$$\begin{aligned}\|\Xi_i - \Xi_i^\star\|_{L^2(\Omega)} \quad \leq \quad & \max_{t\in\Omega}\left|\frac{\beta(t)\eta_i}{\Gamma(\alpha(t))}\sqrt{\frac{r\Gamma(2\alpha(t)-1)\Gamma(2\beta(t)-1)}{\Gamma(2\alpha(t)+2\beta(t)-2)}}t^{\alpha(t)+\beta(t)-\frac{3}{2}}\right| \\ & \left(\eta_i\sqrt{r}\left(\sum_{j=1}^{r}c^2(M-1)^{-2\tau}(2^{k-1})^{-2\tau}\|\Xi_j^{(\tau)}\|^2_{L^2(\Omega)}\right)^{\frac{1}{2}} + \|\mathcal{R}_i\|_{L^2(\Omega)}\right).\end{aligned} \tag{57}$$

Therefore, we conclude that

$$\begin{aligned}\|Total\ Error\|_{L^2(\Omega)} \quad \leq \quad & \max_{1\leq i\leq r}\left(\max_{t\in\Omega}\left|\frac{\beta(t)\eta_i}{\Gamma(\alpha(t))}\sqrt{\frac{r\Gamma(2\alpha(t)-1)\Gamma(2\beta(t)-1)}{\Gamma(2\alpha(t)+2\beta(t)-2)}}t^{\alpha(t)+\beta(t)-\frac{3}{2}}\right|\right. \\ & \left.\left(\eta_i\sqrt{r}\left(\sum_{j=1}^{r}c^2(M-1)^{-2\tau}(2^{k-1})^{-2\tau}\|\Xi_j^{(\tau)}\|^2_{L^2(\Omega)}\right)^{\frac{1}{2}} + \|\mathcal{R}_i\|_{L^2(\Omega)}\right)\right),\end{aligned} \tag{58}$$

which completes the proof. □

Remark 2. *We can obtain the error upper bound for the numerical solution obtained in the Atangana-Riemann-Liouville sense with a similar way for the Caputo sense.*

6 Numerical results and discussion

In this section, we apply three examples to demonstrate the efficiency and accuracy of the mentioned scheme. Also, the computations were performed on a personal computer and the codes were written in Mathematica 10.

Example 1. *([30]) Consider the following system of VFFDEs:*

$$\begin{cases} {}_0\mathcal{D}_t^{\alpha(t),\beta(t)}\Xi_1(t) = (20\zeta+40)(\Xi_2(t)-\Xi_1(t)) + \frac{5\zeta+4}{25}\Xi_1(t)\Xi_3(t), \\ {}_0\mathcal{D}_t^{\alpha(t),\beta(t)}\Xi_2(t) = (55-90\zeta)\Xi_1(t) + (5\zeta+20)\Xi_2(t) - \Xi_1(t)\Xi_3(t), \\ {}_0\mathcal{D}_t^{\alpha(t),\beta(t)}\Xi_3(t) = -\frac{13}{20}\Xi_1^2(t) + \Xi_1(t)\Xi_2(t) + \frac{11-6\zeta}{6}\Xi_3(t), \end{cases} \tag{59}$$

with the initial conditions

$$\Xi_1(0) = 2, \qquad \Xi_2(0) = 1, \qquad \Xi_3(0) = 4,$$

where $\zeta = 0$, $\alpha(t) = \tanh(t+5)$ *and* $\beta(t) = 0.98$. *Now, we explain the mentioned technique in section 4 for the aforesaid problem with* $k = 2, M = 8, \theta = \frac{1}{4}, h = 1$.

Step 1. We approximate the fractal-fractional terms ${}_0\mathcal{D}_t^{\alpha(t),\beta(t)}\Xi_i(t), i = 1, 2, 3,$ *by the FALWs as*

$$\begin{aligned} {}^{CFF}_{0}D_t^{\tanh(t+5),0.98}\Xi_1(t) \quad &\simeq \quad \sum_{n=1}^{2}\sum_{m=0}^{7}c_{n,m}^{(1)}\psi_{n,m,\hat{m}}^{(\frac{1}{4})}(t) = C_1^T\Psi^{(\frac{1}{4})}(t), \\ {}^{CFF}_{0}D_t^{\tanh(t+5),0.98}\Xi_2(t) \quad &\simeq \quad \sum_{n=1}^{2}\sum_{m=0}^{7}c_{n,m}^{(2)}\psi_{n,m,\hat{m}}^{(\frac{1}{4})}(t) = C_2^T\Psi^{(\frac{1}{4})}(t), \\ {}^{CFF}_{0}D_t^{\tanh(t+5),0.98}\Xi_3(t) \quad &\simeq \quad \sum_{n=1}^{2}\sum_{m=0}^{7}c_{n,m}^{(3)}\psi_{n,m,\hat{m}}^{(\frac{1}{4})}(t) = C_3^T\Psi^{(\frac{1}{4})}(t). \end{aligned} \tag{60}$$

Step 2. With the help of the variable-order fractal-fractional integral operator (20) and relation (60), along with the expressed initial conditions, we can approximate the unknown functions $\Xi_i(t), i = 1, 2, 3$ *as*

$$\begin{aligned} \Xi_1(t) \quad &\simeq \quad \Upsilon(t, \tanh(t+5), 0.98, \frac{1}{4}) + 2, \\ \Xi_2(t) \quad &\simeq \quad \Upsilon(t, \tanh(t+5), 0.98, \frac{1}{4}) + 1, \\ \Xi_3(t) \quad &\simeq \quad \Upsilon(t, \tanh(t+5), 0.98, \frac{1}{4}) + 4. \end{aligned} \tag{61}$$

Step 3. By substituting the approximations (60)-(61) into relation (59), we get

$$\begin{cases} \sum_{n=1}^{2}\sum_{m=0}^{7} c_{n,m}^{(1)}\psi_{n,m,\hat{m}}^{(\frac{1}{4})}(t) = (20\zeta+40)((\Upsilon(t,\tanh(t+5),0.98,\frac{1}{4})+1) \\ -(\Upsilon(t,\tanh(t+5),0.98,\frac{1}{4})+2)) \\ +\frac{5\zeta+4}{25}(\Upsilon(t,\tanh(t+5),0.98,\frac{1}{4})+2)(\Upsilon(t,\tanh(t+5),0.98,\frac{1}{4})+4), \\ \sum_{n=1}^{2}\sum_{m=0}^{7} c_{n,m}^{(2)}\psi_{n,m,\hat{m}}^{(\frac{1}{4})}(t) = (55-90\zeta)(\Upsilon(t,\tanh(t+5),0.98,\frac{1}{4})+2) \\ +(5\zeta+20)(\Upsilon(t,\tanh(t+5),0.98,\frac{1}{4})+1) \\ -(\Upsilon(t,\tanh(t+5),0.98,\frac{1}{4})+2)(\Upsilon(t,\tanh(t+5),0.98,\frac{1}{4})+4), \\ \sum_{n=1}^{2}\sum_{m=0}^{7} c_{n,m}^{(3)}\psi_{n,m,\hat{m}}^{(\frac{1}{4})}(t) = -\frac{13}{20}(\Upsilon(t,\tanh(t+5),0.98,\frac{1}{4})+2)^2(t) \\ +(\Upsilon(t,\tanh(t+5),0.98,\frac{1}{4})+2)(\Upsilon(t,\tanh(t+5),0.98,\frac{1}{4})+1) \\ +\frac{11-6\zeta}{6}(\Upsilon(t,\tanh(t+5),0.98,\frac{1}{4})+4). \end{cases} \tag{62}$$

Step 4. We define the residual functions $\mathcal{R}_i(t), i=1,2,3$ *as*

$$\begin{cases} \mathcal{R}_1(t) = \sum_{n=1}^{2}\sum_{m=0}^{7} c_{n,m}^{(1)}\psi_{n,m,\hat{m}}^{(\frac{1}{4})}(t) - (20\zeta+40)((\Upsilon(t,\tanh(t+5),0.98,\frac{1}{4})+1) \\ -(\Upsilon(t,\tanh(t+5),0.98,\frac{1}{4})+2)) \\ -\frac{5\zeta+4}{25}(\Upsilon(t,\tanh(t+5),0.98,\frac{1}{4})+2)(\Upsilon(t,\tanh(t+5),0.98,\frac{1}{4})+4), \\ \mathcal{R}_2(t) = \sum_{n=1}^{2}\sum_{m=0}^{7} c_{n,m}^{(2)}\psi_{n,m,\hat{m}}^{(\frac{1}{4})}(t) - (55-90\zeta)(\Upsilon(t,\tanh(t+5),0.98,\frac{1}{4})+2) \\ -(5\zeta+20)(\Upsilon(t,\tanh(t+5),0.98,\frac{1}{4})+1) \\ +(\Upsilon(t,\tanh(t+5),0.98,\frac{1}{4})+2)(\Upsilon(t,\tanh(t+5),0.98,\frac{1}{4})+4), \\ \mathcal{R}_3(t) = \sum_{n=1}^{2}\sum_{m=0}^{7} c_{n,m}^{(3)}\psi_{n,m,\hat{m}}^{(\frac{1}{4})}(t) + \frac{13}{20}(\Upsilon(t,\tanh(t+5),0.98,\frac{1}{4})+2)^2(t) \\ -(\Upsilon(t,\tanh(t+5),0.98,\frac{1}{4})+2)(\Upsilon(t,\tanh(t+5),0.98,\frac{1}{4})+1) \\ -\frac{11-6\zeta}{6}(\Upsilon(t,\tanh(t+5),0.98,\frac{1}{4})+4), \end{cases} \tag{63}$$

Step 5. By collocating the system (63) at the zeros of the shifted Legendre polynomials, we achieve

$$\begin{cases} \mathcal{R}_1(t_\iota) = 0, \\ \mathcal{R}_2(t_\iota) = 0, \\ \mathcal{R}_3(t_\iota) = 0, \end{cases} \tag{64}$$

$$\iota = 1, 2, \ldots, 16.$$

So, we achieve a system of 48 nonlinear algebraic equations with 48 unknown coefficients, which can be solved via the Newton's iterative method.

Table 1 describes the numerical results (NRs) and error estimation (EE) of the presented technique for $k=2, M=8, \theta=\frac{1}{4}, h=1$ *with CFF and ARLFF via the FALWs. A comparison of the EE for* $k=2, M=8, h=1$ *and diverse values of* θ *with ARLFF are provided in Table 2. Also, in Table 3 we compared the EE where* $\theta=\frac{1}{8}, h=1$ *for different values of* k, M *with CFF. In addition, the CPU time (in seconds) is reported in Tables 2 and 3. From Table 3, it can be inferred that using more number of the FALWs, we can obtain a numerical solution with high precision. The behavior of the numerical solutions for* $k=2, M=6, h=2, \theta=\frac{1}{4}$ *and* $\beta(t)\in(0,1)$ *with CFFP is plotted in Figure 4. We have reported the EE with* $k=2, M=8, h=2, \theta=\frac{1}{8}$ *for the CFF and ARLFF in Figure 5. Moreover, the NR for* $k=1, h=10, \theta=\frac{1}{8}$ *and* $M=4,6,8$ *with ARLFF is denoted in Figure 6.*

Example 2. *([30]) Consider the following system of VFFDEs:*

$$\begin{cases} {}_0\mathcal{D}_t^{\alpha(t),\beta(t)}\Xi_1(t) = -(\Xi_3(t)+\Xi_2(t)), \\ {}_0\mathcal{D}_t^{\alpha(t),\beta(t)}\Xi_2(t) = \Xi_1(t)+\zeta_1\Xi_2(t), \\ {}_0\mathcal{D}_t^{\alpha(t),\beta(t)}\Xi_3(t) = \zeta_2+\Xi_3(t)(\Xi_1(t)-\zeta_3), \end{cases} \tag{65}$$

with the initial conditions

$$\Xi_1(0) = 4.87623, \qquad \Xi_2(0) = 4.87623, \qquad \Xi_3(0) = 0.1278,$$

Table 1: The NRs and EE of the established method with $k = 2, M = 8, \theta = \frac{1}{4}, h = 1$ for CFF and ARLFF in Example 1.

t	CFF				ARLFF			
	$\Xi_1(t)$	$\Xi_2(t)$	$\Xi_3(t)$	EE	$\Xi_1(t)$	$\Xi_2(t)$	$\Xi_3(t)$	EE
0.1	2.35443	1.12868	4.41065	2.46×10^{-6}	2.28395	1.70568	4.31898	7.55×10^{-6}
0.2	2.68348	1.23623	4.80391	3.64×10^{-7}	2.58969	2.11993	4.58839	1.17×10^{-6}
0.3	2.99373	1.32533	5.18713	1.00×10^{-6}	2.87241	2.57668	4.83341	3.18×10^{-6}
0.4	3.28664	1.39662	5.56185	3.00×10^{-6}	3.13367	3.07588	5.05528	9.15×10^{-6}
0.5	3.56290	1.45045	5.92883	2.95×10^{-5}	3.37423	3.61756	5.25464	8.49×10^{-5}
0.6	4.50217	1.98455	6.59573	6.01×10^{-5}	3.73602	4.31904	5.36074	3.84×10^{-5}
0.7	5.53107	2.57940	7.24276	1.40×10^{-6}	4.03903	4.90139	5.44501	1.07×10^{-6}
0.8	6.64956	3.23492	7.87036	2.63×10^{-7}	4.33406	5.50965	5.51736	3.96×10^{-8}
0.9	7.85755	3.95101	8.47885	2.69×10^{-7}	4.62121	6.14348	5.57785	1.56×10^{-8}

Table 2: Comparison of the EE with $k = 2, M = 8, h = 1$ and diverse values of θ for ARLFF in Example 1.

t	$\theta = \frac{1}{8}$	$\theta = \frac{1}{5}$	$\theta = \frac{1}{4}$	$\theta = \frac{1}{2}$	$\theta = \frac{2}{3}$	$\theta = 1$
0.1	2.54×10^{-5}	1.25×10^{-5}	7.55×10^{-6}	3.39×10^{-4}	4.64×10^{-3}	3.78×10^{1}
0.2	2.55×10^{-6}	1.72×10^{-6}	1.17×10^{-6}	1.05×10^{-4}	5.81×10^{-3}	3.78×10^{1}
0.3	5.40×10^{-6}	4.41×10^{-6}	3.18×10^{-6}	5.14×10^{-4}	6.49×10^{-2}	3.78×10^{1}
0.4	1.32×10^{-5}	1.22×10^{-5}	9.15×10^{-6}	2.49×10^{-3}	5.95×10^{-1}	3.78×10^{1}
0.5	1.08×10^{-4}	1.11×10^{-3}	8.49×10^{-5}	3.71×10^{-2}	1.52×10^{1}	3.77×10^{1}
0.6	1.88×10^{-5}	2.98×10^{-5}	3.84×10^{-5}	7.44×10^{-4}	1.76×10^{-1}	3.78×10^{1}
0.7	2.53×10^{-6}	8.96×10^{-7}	1.07×10^{-6}	2.98×10^{-4}	1.78×10^{-1}	3.79×10^{1}
0.8	6.02×10^{-9}	3.27×10^{-8}	3.96×10^{-8}	1.30×10^{-6}	1.56×10^{-3}	3.81×10^{1}
0.9	2.64×10^{-9}	1.76×10^{-8}	1.56×10^{-8}	5.32×10^{-7}	1.23×10^{-3}	3.85×10^{1}
CPU times	1.750	2.728	2.906	2.922	5.656	5.203

Table 3: Comparison of the EE with $\theta = \frac{1}{8}, h = 1$ and diverse values of k, M for the CFF in Example 1.

t	$k = 1$				$k = 2$			
	$M = 2$	$M = 4$	$M = 6$	$M = 8$	$M = 2$	$M = 4$	$M = 6$	$M = 8$
0.1	1.62×10^{-1}	1.21×10^{-1}	4.40×10^{-3}	2.44×10^{-5}	7.09×10^{-1}	2.29×10^{-3}	1.24×10^{-4}	7.98×10^{-6}
0.2	9.80×10^{-2}	7.94×10^{-2}	4.10×10^{-4}	4.09×10^{-5}	1.09×10^{-1}	1.69×10^{-2}	1.33×10^{-5}	8.45×10^{-7}
0.3	5.00×10^{-1}	1.15×10^{-2}	2.54×10^{-4}	1.37×10^{-5}	3.29×10^{-1}	2.16×10^{-2}	2.42×10^{-5}	1.82×10^{-6}
0.4	7.03×10^{-1}	1.46×10^{-2}	3.26×10^{-5}	7.54×10^{-7}	8.81×10^{-1}	4.91×10^{-3}	7.81×10^{-5}	4.74×10^{-6}
0.5	6.87×10^{-1}	1.60×10^{-2}	6.85×10^{-5}	3.35×10^{-6}	2.30×10^{-1}	9.19×10^{-2}	4.21×10^{-4}	4.08×10^{-5}
0.6	5.30×10^{-1}	7.04×10^{-3}	1.04×10^{-5}	1.71×10^{-7}	1.88×10^{-1}	1.54×10^{-2}	4.38×10^{-4}	8.35×10^{-5}
0.7	2.80×10^{-1}	2.56×10^{-3}	2.40×10^{-5}	6.41×10^{-7}	3.83×10^{-1}	1.36×10^{-2}	9.20×10^{-6}	1.12×10^{-6}
0.8	3.89×10^{-2}	7.14×10^{-3}	9.44×10^{-6}	3.03×10^{-7}	7.34×10^{-1}	2.51×10^{-3}	4.51×10^{-7}	1.76×10^{-7}
0.9	4.08×10^{-1}	3.22×10^{-3}	1.50×10^{-5}	1.34×10^{-8}	2.52×10^{-1}	6.20×10^{-5}	2.40×10^{-7}	1.92×10^{-7}
CPU times	0.001	0.031	0.063	0.125	0.031	0.078	0.515	1.531

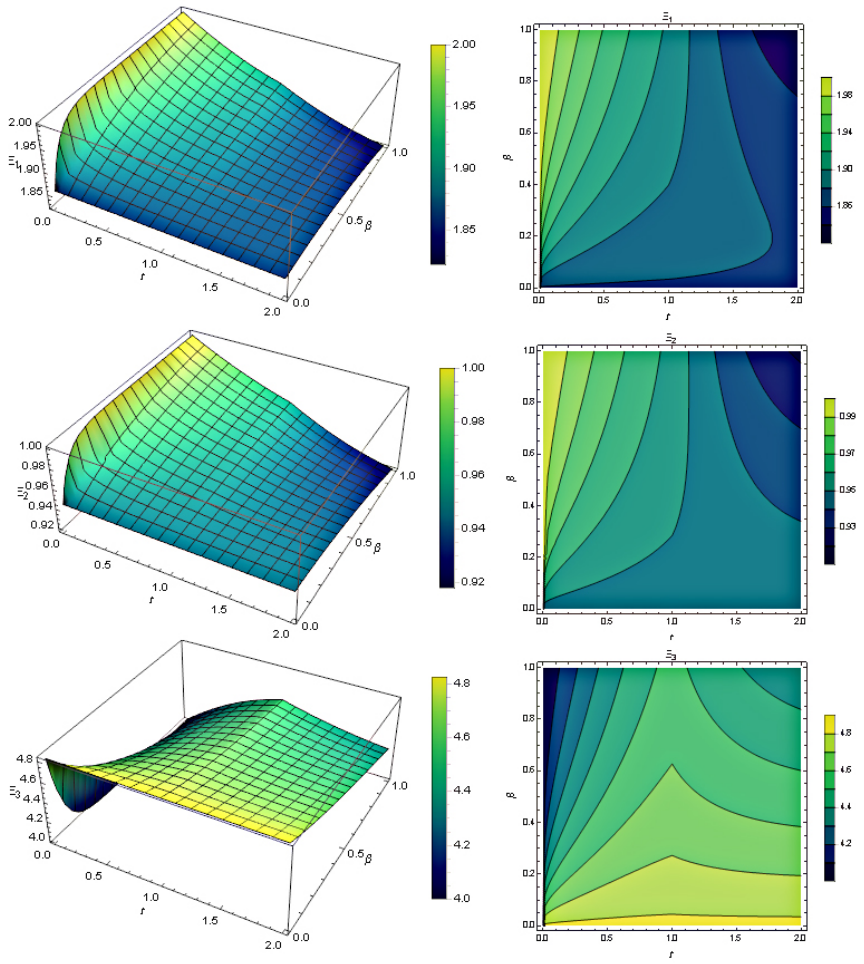

Figure 4: The NR with $k = 2, M = 6, h = 2, \theta = \frac{1}{4}$ and $\beta(t) \in (0, 1)$ for the CFFP in Example 1.

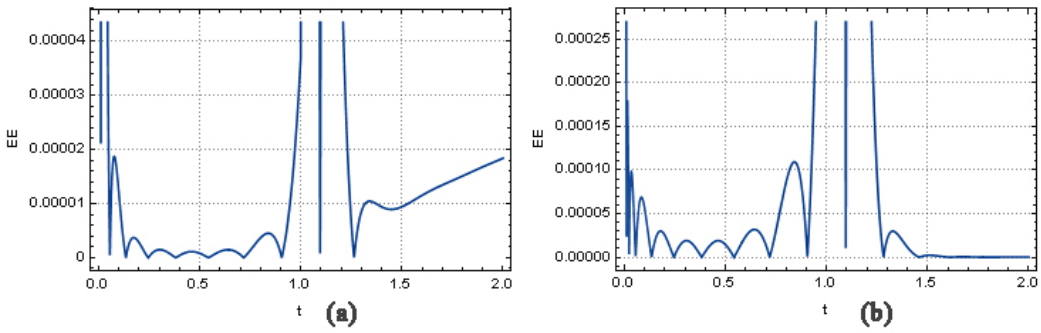

Figure 5: The EE with $k = 2, M = 8, h = 2, \theta = \frac{1}{8}$ for (a) : CFF and (b) : ARLFF in Example 1.

where $\zeta_1 = \zeta_2 = 0.1$, $\zeta_3 = 14$ *and* $\beta(t) = 0.99 + \frac{0.01}{2}(\sin(t) + 1)$. *We have reported the NRs and EE obtained from the proposed method with* $k = 2, M = 9, \theta = \frac{1}{8}, h = 1$ *for the CFF and ARLFF in Table 4. Table 5 contains the EE and CPU time obtained by the mentioned scheme with* $k = 2, M = 9, h = 1$ *and different values of* θ *for the ARLFF. From this table, it can be observed that the best value for* θ *is* $\frac{1}{4}$. *Also, the EE and CPU time with* $\theta = \frac{1}{8}, h = 1$ *and different values of* k, M *for the CFF are illustrated in Table 6. This table illustrates that as the number of FALWs increases, the numerical solutions converge to the exact solution. The numerical solutions with* $k = 2, M = 9, h = 2$ *and* $\alpha(t) \in (0, 1)$ *for* $\theta = 1$ *and* $\theta = \frac{1}{8}$ *are plotted in Figures 7 and*

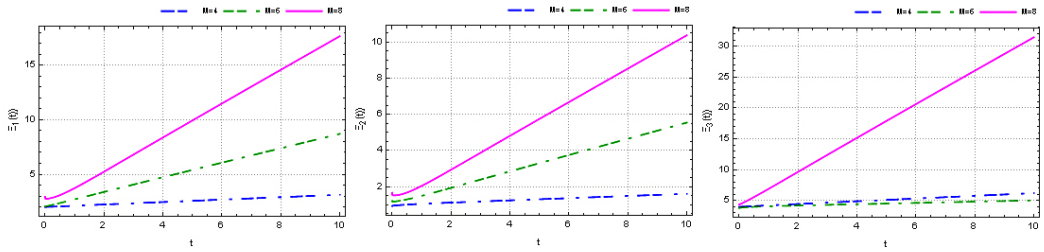

Figure 6: The NR with $k = 1, h = 10, \theta = \frac{1}{8}$ and $M = 4, 6, 8$ for the ARLFF in Example 1.

8, respectively. Figure 9 demonstrates the EE with $k = 2, M = 9, h = 2, \theta = \frac{1}{8}$ *for the CFF and ARLFF. Also, the NRs are depicted graphically with* $k = 1, h = 200, \theta = 1$ *and* $M = 5, 7, 9$ *for the CFF and ARLFF in Figure 10.*

Table 4: The NRs and EE of the established method with $k = 2, M = 9, \theta = \frac{1}{8}, h = 1$ for the CFF and ARLFF in Example 2.

t	CFF				ARLFF			
	$\Xi_1(t)$	$\Xi_2(t)$	$\Xi_3(t)$	EE	$\Xi_1(t)$	$\Xi_2(t)$	$\Xi_3(t)$	EE
0.1	4.68704	5.51386	0.15816	3.49×10^{-7}	0.497225	6.56744	0.00165	4.58×10^{-9}
0.2	4.50482	6.12825	0.18699	1.46×10^{-6}	−0.00755	7.00514	0.00069	4.53×10^{-9}
0.3	4.32529	6.73386	0.21501	3.36×10^{-6}	−0.51365	7.43899	− 0.00046	4.46×10^{-9}
0.4	4.14750	7.33380	0.24236	6.04×10^{-6}	−1.01959	7.86994	− 0.00167	3.74×10^{-8}
0.5	3.97102	7.92961	0.26913	8.92×10^{-6}	−1.52525	8.29866	− 0.00292	3.66×10^{-7}
0.6	3.75236	8.59992	0.29363	5.67×10^{-6}	6.50310	− 1.79384	0.01641	4.31×10^{-7}
0.7	3.52998	9.27689	0.31755	4.86×10^{-6}	6.97981	− 1.68351	0.01702	2.33×10^{-9}
0.8	3.30313	9.96203	0.34090	2.15×10^{-6}	7.45905	− 1.57520	0.01758	1.75×10^{-8}
0.9	3.07162	10.6558	0.36368	8.77×10^{-7}	7.94346	− 1.46915	0.018085	3.34×10^{-8}

Table 5: Comparison of the EE with $k = 2, M = 9, h = 1$ and different values of θ for the ARLFF in Example 2.

t	$\theta = \frac{1}{8}$	$\theta = \frac{1}{4}$	$\theta = \frac{1}{3}$	$\theta = \frac{1}{2}$	$\theta = \frac{2}{3}$	$\theta = 1$
0.1	4.58×10^{-9}	1.06×10^{-9}	3.82×10^{-1}	7.98×10^{-8}	1.10×10^{-2}	3.49×10^{-6}
0.2	4.53×10^{-9}	2.42×10^{-9}	3.82×10^{-1}	3.17×10^{-7}	6.04×10^{-6}	2.76×10^{-5}
0.3	4.46×10^{-9}	8.20×10^{-10}	3.82×10^{-1}	1.56×10^{-7}	3.67×10^{-6}	2.18×10^{-5}
0.4	3.74×10^{-8}	9.26×10^{-9}	3.82×10^{-1}	2.17×10^{-6}	5.92×10^{-5}	4.37×10^{-4}
0.5	3.66×10^{-7}	1.45×10^{-7}	3.82×10^{-1}	4.22×10^{-5}	1.30×10^{-3}	1.15×10^{-2}
0.6	4.31×10^{-7}	8.97×10^{-8}	3.82×10^{-1}	2.33×10^{-8}	1.01×10^{-5}	2.35×10^{-5}
0.7	2.33×10^{-9}	5.59×10^{-10}	3.82×10^{-1}	4.01×10^{-10}	9.56×10^{-8}	4.01×10^{-7}
0.8	1.75×10^{-8}	2.73×10^{-10}	3.82×10^{-1}	3.19×10^{-10}	2.60×10^{-8}	1.44×10^{-7}
0.9	3.34×10^{-8}	2.58×10^{-10}	3.82×10^{-1}	4.10×10^{-10}	1.69×10^{-9}	3.05×10^{-9}
CPU times	1.516	2.484	0.797	6.156	1.438	1.672

Example 3. *([30]) Consider the following system VFFDE:*

$$\begin{cases} {}_0\mathcal{D}_t^{\alpha(t),\beta(t)}\Xi_1(t) = \Xi_2(t), \\ {}_0\mathcal{D}_t^{\alpha(t),\beta(t)}\Xi_2(t) = -(\zeta_1 + \zeta_2\Xi_3(t))\Xi_1(t) - (\zeta_1 + \zeta_2\Xi_3(t))\Xi_1^3(t) - \zeta_3\Xi_2(t) + \zeta_4\Xi_3(t), \\ {}_0\mathcal{D}_t^{\alpha(t),\beta(t)}\Xi_3(t) = \Xi_4(t), \\ {}_0\mathcal{D}_t^{\alpha(t),\beta(t)}\Xi_4(t) = -\Xi_3(t) + \zeta_5(1 - \Xi_3^2(t))\Xi_4(t) + \zeta_6\Xi_1(t), \end{cases} \tag{66}$$

with the initial conditions $\Xi_1(0) = \Xi_2(0) = \Xi_3(0) = \Xi_4(0) = 0$, *where* $\zeta_1 = 10, \zeta_2 = 3, \zeta_3 = 0.4, \zeta_4 = 70, \zeta_5 = 5, \zeta_6 = 0.1, \alpha(t) = \tanh(t + 5), \beta(t) = 0.99 + \frac{0.01}{2}(\sin(t) + 1)$. *The NRs and EE of the presented method with* $k = 2, M = 8, \theta = \frac{1}{8}, h = 1$ *for the CFF and ARLFF are considered*

Table 6: Comparison of the EE with $\theta = \frac{1}{8}, h = 1$ and different values of k, M for the CFF in Example 2.

t	$k=1$				$k=2$			
	$M=3$	$M=5$	$M=7$	$M=9$	$M=3$	$M=5$	$M=7$	$M=9$
0.1	1.73×10^{-2}	8.56×10^{-3}	1.60×10^{-4}	5.80×10^{-5}	6.58×10^{-2}	6.08×10^{-4}	1.91×10^{-6}	3.49×10^{-7}
0.2	4.02×10^{-2}	9.43×10^{-4}	4.78×10^{-5}	1.68×10^{-6}	2.07×10^{-2}	2.41×10^{-4}	9.28×10^{-7}	1.46×10^{-6}
0.3	3.18×10^{-2}	7.42×10^{-4}	8.22×10^{-7}	1.74×10^{-6}	3.74×10^{-2}	9.68×10^{-5}	8.09×10^{-7}	3.36×10^{-6}
0.4	1.46×10^{-2}	4.54×10^{-4}	8.01×10^{-6}	8.01×10^{-7}	1.47×10^{-2}	2.21×10^{-4}	1.65×10^{-6}	6.04×10^{-6}
0.5	1.99×10^{-4}	3.36×10^{-6}	6.70×10^{-8}	6.87×10^{-9}	1.20×10^{-1}	1.52×10^{-3}	1.04×10^{-5}	8.92×10^{-6}
0.6	8.90×10^{-3}	1.78×10^{-4}	2.74×10^{-6}	1.71×10^{-7}	1.88×10^{-2}	1.08×10^{-3}	1.87×10^{-5}	5.67×10^{-6}
0.7	1.15×10^{-2}	1.08×10^{-4}	8.91×10^{-8}	7.08×10^{-8}	1.52×10^{-2}	6.17×10^{-5}	6.71×10^{-7}	4.86×10^{-6}
0.8	7.91×10^{-3}	4.32×10^{-5}	1.35×10^{-6}	1.05×10^{-8}	3.29×10^{-3}	2.47×10^{-5}	6.96×10^{-8}	2.15×10^{-6}
0.9	1.50×10^{-3}	8.32×10^{-5}	7.19×10^{-7}	2.52×10^{-8}	3.25×10^{-3}	7.07×10^{-6}	7.68×10^{-9}	8.77×10^{-7}
CPU times	0.016	0.125	0.175	0.235	0.063	0.256	0.500	1.672

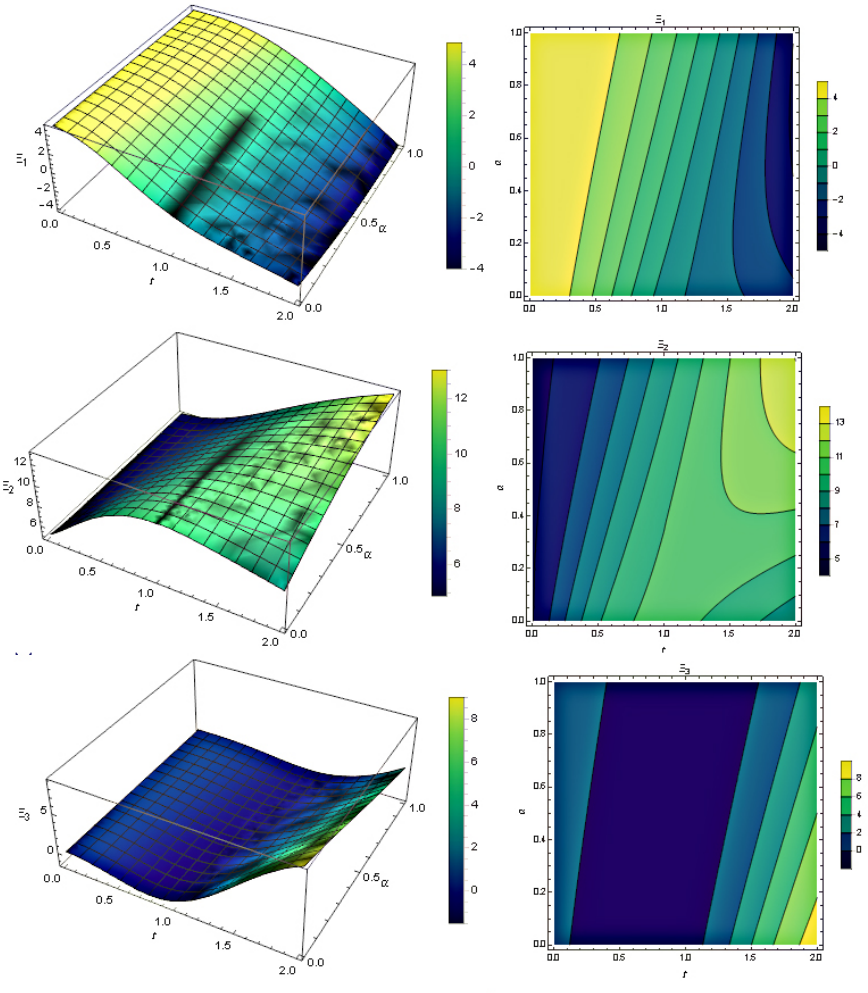

Figure 7: The NR with $k = 2, M = 9, h = 2, \theta = 1$ and $\alpha(t) \in (0, 1)$ for CFF in Example 2.

in Table 7. Comparison of the EE and CPU time with $k = 2, M = 8, h = 1$ and different values of θ for the CFF and ARLFF are shown in Tables 8 and 9. Also, in Table 10, we compare the EE and CPU time obtained by the presented strategy with $\theta = \frac{1}{8}, h = 1$ and different values of k, M. We plot the approximate solutions for $k = 1$ with the CFF ($h = 1, \theta = 1$) and ARLFF ($h = 400, \theta = \frac{2}{3}, 1$) in Figures 11 and 12, respectively.

Table 7: The NRs and EE of the established method with $k = 2, M = 8, \theta = \frac{1}{8}, h = 1$ for the CFF and ARLFF in Example 3.

t	CFF					ARLFF				
	$\Xi_1(t)$	$\Xi_2(t)$	$\Xi_3(t)$	$\Xi_4(t)$	EE	$\Xi_1(t)$	$\Xi_2(t)$	$\Xi_3(t)$	$\Xi_4(t)$	EE
0.1	1.45517	1.88902	1.50680	1.78742	1.43×10^{-7}	1.46826	2.16717	1.50842	1.82503	6.44×10^{-7}
0.2	1.41069	2.27493	1.51354	2.07255	1.50×10^{-8}	1.42835	2.64171	1.51499	2.15518	6.00×10^{-8}
0.3	1.36633	2.65978	1.52027	2.35689	1.95×10^{-8}	1.38881	3.12043	1.52160	2.48420	1.52×10^{-7}
0.4	1.32204	3.04410	1.52699	2.64084	5.14×10^{-8}	1.34951	3.60286	1.52824	2.81258	3.41×10^{-7}
0.5	1.27778	3.42818	1.53370	2.92461	2.86×10^{-7}	1.31040	4.08851	1.53491	3.14061	2.99×10^{-6}
0.6	1.23613	3.85288	1.51490	3.26210	7.52×10^{-6}	1.33267	5.42140	1.53175	3.04058	3.10×10^{-5}
0.7	1.19447	4.27763	1.49610	3.59961	1.43×10^{-7}	1.30768	6.57633	1.53569	3.08303	5.59×10^{-7}
0.8	1.15281	4.70251	1.47730	3.93723	2.89×10^{-8}	1.28408	7.73849	1.53946	3.12146	1.59×10^{-8}
0.9	1.11112	5.12757	1.45850	4.27499	3.91×10^{-8}	1.26163	8.90675	1.54308	3.15664	1.73×10^{-8}

Table 8: Comparison of the EE with $k = 2, M = 8, h = 1$ and different values of θ for the CFF in Example 3.

t	$\theta = \frac{1}{8}$	$\theta = \frac{1}{5}$	$\theta = \frac{1}{3}$	$\theta = \frac{2}{3}$	$\theta = 1$
0.1	1.43×10^{-7}	3.31×10^{-8}	3.62×10^{-7}	9.83×10^{-6}	7.94×10^{-1}
0.2	1.50×10^{-8}	3.31×10^{-9}	7.40×10^{-7}	3.76×10^{-6}	7.94×10^{-1}
0.3	1.95×10^{-8}	1.97×10^{-8}	1.04×10^{-6}	1.89×10^{-5}	7.94×10^{-1}
0.4	5.14×10^{-8}	3.91×10^{-8}	1.17×10^{-6}	8.88×10^{-5}	7.95×10^{-1}
0.5	2.86×10^{-7}	5.05×10^{-7}	3.26×10^{-6}	1.24×10^{-3}	7.90×10^{-1}
0.6	7.52×10^{-6}	2.40×10^{-6}	1.52×10^{-4}	1.29×10^{-4}	8.08×10^{-1}
0.7	1.43×10^{-7}	1.01×10^{-7}	3.55×10^{-4}	5.76×10^{-6}	7.93×10^{-1}
0.8	2.89×10^{-8}	7.31×10^{-8}	6.49×10^{-4}	2.75×10^{-7}	7.95×10^{-1}
0.9	3.91×10^{-8}	1.05×10^{-7}	1.06×10^{-3}	1.34×10^{-7}	7.95×10^{-1}
CPU times	12.296	16.439	2.750	6.844	8.453

Table 9: Comparison of the EE with $k = 2, M = 8, h = 1$ and different values of θ for the ARLFF in Example 3.

t	$\theta = \frac{1}{8}$	$\theta = \frac{1}{5}$	$\theta = \frac{1}{3}$	$\theta = \frac{2}{3}$	$\theta = 1$
0.1	6.44×10^{-7}	4.39×10^{-6}	2.17×10^{-6}	9.79×10^{-6}	2.88×10^{-6}
0.2	6.00×10^{-8}	2.01×10^{-5}	3.27×10^{-6}	3.80×10^{-6}	2.56×10^{-6}
0.3	1.52×10^{-7}	4.73×10^{-5}	2.83×10^{-6}	1.92×10^{-5}	1.93×10^{-5}
0.4	3.41×10^{-7}	8.61×10^{-5}	4.25×10^{-7}	9.04×10^{-5}	1.18×10^{-4}
0.5	2.99×10^{-6}	1.34×10^{-4}	3.38×10^{-6}	1.27×10^{-3}	1.99×10^{-3}
0.6	3.10×10^{-5}	5.45×10^{-4}	2.04×10^{-5}	1.46×10^{-4}	1.42×10^{-3}
0.7	5.59×10^{-7}	1.35×10^{-3}	4.71×10^{-5}	6.54×10^{-6}	1.71×10^{-4}
0.8	1.59×10^{-8}	2.28×10^{-3}	9.12×10^{-5}	3.12×10^{-7}	1.58×10^{-5}
0.9	1.73×10^{-8}	3.33×10^{-3}	1.51×10^{-4}	1.53×10^{-7}	1.27×10^{-5}
CPU times	15.906	2.922	3.334	8.281	10.109

Table 10: Comparison of the EE with $\theta = \frac{1}{8}, h = 1$ and different values of k, M for the CFF in Example 3.

t	$k = 1$				$k = 2$			
	$M = 2$	$M = 4$	$M = 6$	$M = 8$	$M = 2$	$M = 4$	$M = 6$	$M = 8$
0.1	7.41×10^{-2}	6.00×10^{-3}	2.49×10^{-4}	4.60×10^{-6}	3.83×10^{-2}	1.11×10^{-4}	1.50×10^{-5}	1.43×10^{-7}
0.2	4.53×10^{-3}	4.05×10^{-3}	2.15×10^{-5}	8.83×10^{-6}	6.00×10^{-2}	8.31×10^{-4}	1.86×10^{-6}	1.50×10^{-8}
0.3	2.34×10^{-2}	6.01×10^{-4}	1.21×10^{-5}	3.27×10^{-6}	1.85×10^{-2}	1.08×10^{-3}	3.74×10^{-6}	1.95×10^{-8}
0.4	3.32×10^{-2}	7.71×10^{-4}	1.36×10^{-6}	1.93×10^{-7}	5.03×10^{-2}	2.49×10^{-4}	1.32×10^{-5}	5.14×10^{-8}
0.5	3.28×10^{-2}	8.53×10^{-4}	2.42×10^{-6}	6.43×10^{-7}	1.34×10^{-1}	4.71×10^{-3}	7.72×10^{-5}	2.86×10^{-7}
0.6	2.55×10^{-2}	3.80×10^{-4}	2.94×10^{-7}	4.99×10^{-8}	5.53×10^{-2}	7.64×10^{-4}	5.57×10^{-5}	7.52×10^{-6}
0.7	1.36×10^{-2}	1.40×10^{-4}	4.96×10^{-7}	1.96×10^{-7}	1.13×10^{-2}	6.86×10^{-4}	1.19×10^{-6}	1.43×10^{-7}
0.8	1.91×10^{-3}	3.93×10^{-4}	1.20×10^{-7}	9.46×10^{-8}	2.16×10^{-2}	1.29×10^{-4}	5.74×10^{-8}	2.89×10^{-8}
0.9	2.01×10^{-2}	1.79×10^{-4}	6.32×10^{-8}	5.29×10^{-9}	7.41×10^{-3}	3.22×10^{-6}	2.91×10^{-8}	3.91×10^{-8}
CPU times	0.016	0.047	0.188	0.375	0.047	0.203	0.892	12.296

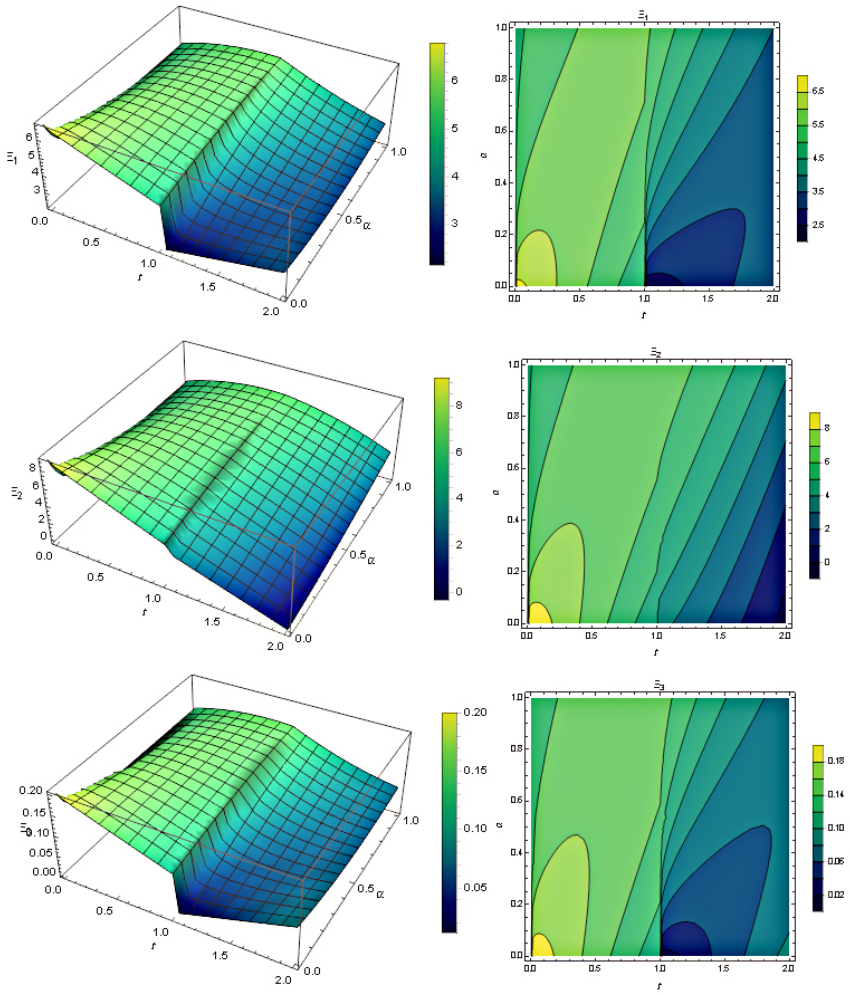

Figure 8: The NR with $k = 2, M = 9, h = 2, \theta = \frac{1}{8}$ and $\alpha(t) \in (0, 1)$ for the CFF in Example 2.

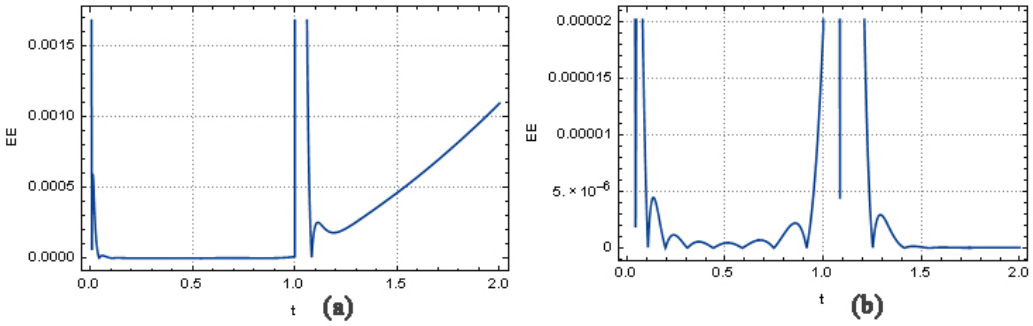

Figure 9: The EE with $k = 2, M = 9, h = 2, \theta = \frac{1}{8}$ for (a) : the CFF and (b) : the ARLFF in Example 2.

7 Conclusions

In this work, a flexible framework based on the FALWs was used for solving systems of VFFDEs associated with the Caputo and Atangana-Riemann-Liouville senses. The exact formula of the variable-order fractal-fractional integral operator of the FALWs was calculated by using the reg-

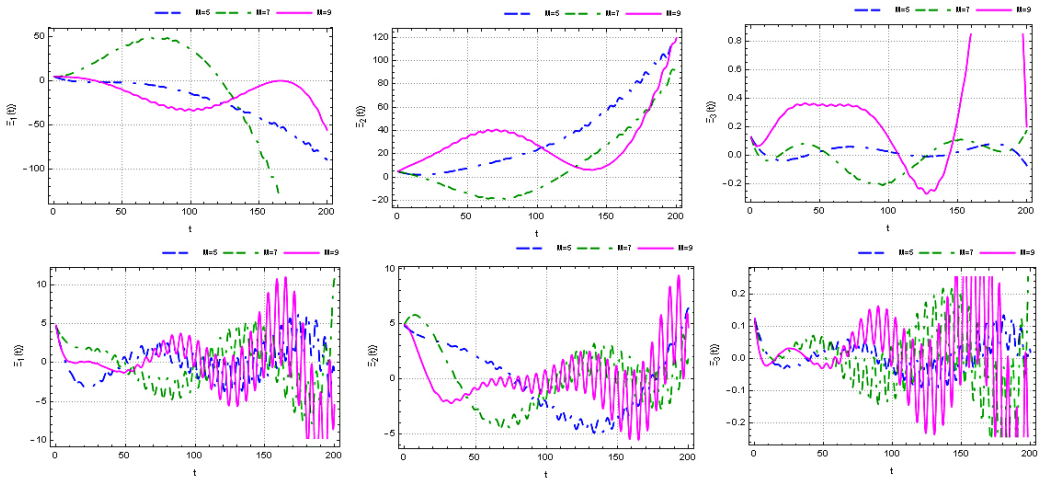

Figure 10: The NR with $k = 1, h = 200, \theta = 1$ and $M = 5, 7, 9$ for up: the CFF and bottom: the ARLFF in Example 2.

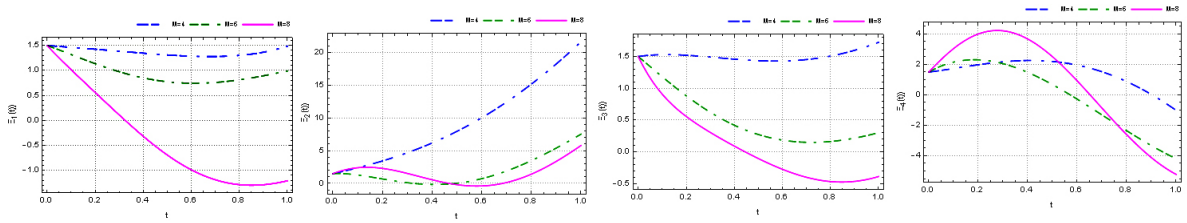

Figure 11: The NR with $\theta = 1$, $k = 1, h = 1$, for the CFF in Example 3.

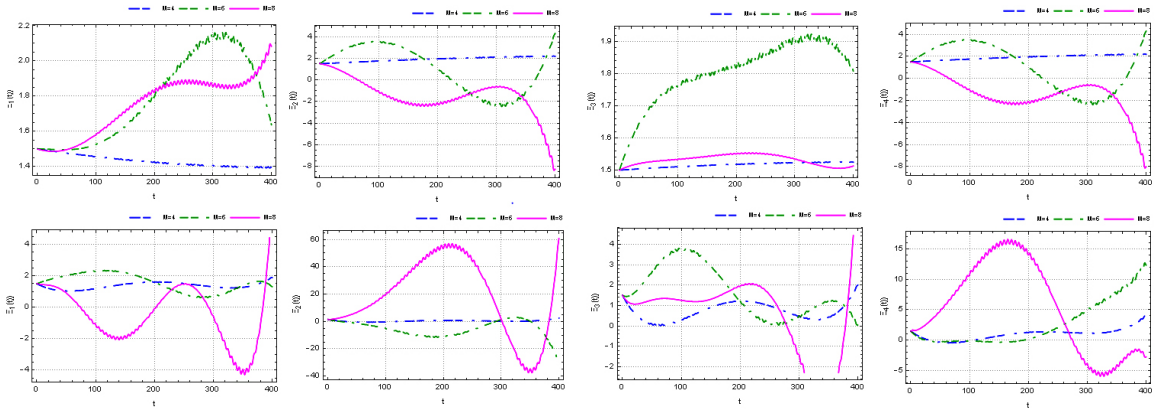

Figure 12: The NR for up: $\theta = \frac{2}{3}$ and bottom: $\theta = 1$ with $k = 1, h = 400$, and ARLFF in Example 3.

ularized beta function. Using a collocation method based on the FALWs, we transformed the problem under consideration to a system of algebraic equations. Also, the error upper bound of the numerical solution in the Sobolev space was discussed. At the end, the approximate results obtained from the established method for some examples confirmed that the expressed scheme is a powerful and efficient tool for solving systems of VFF differential equations. The suggested strategy can be applied to a wider class of biological systems, such as infectious diseases dynamics, finance economics, and engineering problems. We offer the following works in the future:

- This method can be used to solve different problems such as pantograph fractional differential equations, optimal control problems, delay fractal-fractional differential equations, fractal-fractional integro-differential equations etc.
- We can used other wavelets base, including Hahn wavelets, Legendre wavelets, Bernstein wavelets etc.
- We can obtain the variable-order fractal-fractional integral operator of the FALWs by using the Laplace transform method.
- We can applied machine learning method such as neural networks, and least squares-support vector regression for solving the proposed problem.

Acknowledgements

We express our sincere thanks to the anonymous referees for their valuable suggestions that improved the final manuscript.

Contribution statements

Parisa Rahimkhani
Conceptualization, Data curation, Investigation, Software, Writing -original draft
Salameh Sedaghat
Conceptualization, Validation, Writing -review and editing

Declaration of Competing Interest

The authors declare that they have no known competing financial interests or personal relationships that could have appeared to influence the work reported in this paper.

Availability of supporting data

Data will be made available on reasonable request.

References

[1] Lederman C, Roquejoffre JM, Wolanski N (2004) Mathematical justification of a nonlinear integrodifferential equation for the propagation of spherical flames. Annali di Matematica 183:173−239

[2] Kulish VV, Lage JL (2002) Application of fractional calculus to fluid mechanics. J Fluids Eng 124(3):803−806

[3] Bagley RL, Torvik PJ (1985) Fractional calculus in the transient analysis of viscoelastically damped structures. AIAA J 23:918−925

[4] Meral FC, Royston TJ, Magin R (2010) Fractional calculus in viscoelasticity: an experimental study. Commun Nonlinear Sci Numer Simul 15:939−945

[5] Engheta N (1996) On fractional calculus and fractional multipoles in electromagnetism. Antennas Propag 44:554−566

[6] Almeida R, Malinowska AB, Monteiro MTT (2018) Fractional differential equations with a Caputo derivative with respect to a kernel function and their applications. Math Method Appl Sci 41:336−352.

[7] Podlubny I (1999) Fractional differential equations. Academic Press, San Diego.

[8] Rahimkhani P, Ordokhani Y (2020) The bivariate Muntz wavelets composite collocation method for solving space-time fractional partial differential equations. Comput Appl Math 39:115.

[9] Ngo HTB, Vo TN, Razzaghi M (2022) An effective method for solving nonlinear fractional differential equations. Engineering with Computers 38:207−218

[10] Rahimkhani P, Ordokhani Y, Lima PM (2019) An improved composite collocation method for distributed-order fractional differential equations based on fractional Chelyshkov wavelets. Appl Numer Math 145:1−27

[11] Toan PT, Vo TN, Razzaghi M (2019) Taylor wavelet method for fractional delay differential equations. Eng Comput 2019:1–10

[12] Sabermahani S, Ordokhani Y, Yousefi SA (2019) Fractional-order general Lagrange scaling functions and their applications. BIT Numer Math 60:101−128

[13] Rahimkhani P (2023) Numerical solution of nonlinear stochastic differential equations with fractional Brownian motion using fractional-order Genocchi deep neural networks. Communications in Nonlinear Science and Numerical Simulation 126:107466.

[14] Sabermahani S, Ordokhani Y, Rahimkhani P (2024) Touchard-Ritz method to solve variable-order fractional optimal control problems. Iranian Journal of Science and Technology, Transactions of Electrical Engineering 48:1189−1198.

[15] Atangana A (2017) Fractal-fractional differentiation and integration: Connecting fractal calculus and fractional calculus to predict complex system. Chaos Solitons Fractals 102:396−406

[16] Atangana A, Qureshi S (2019) Modeling attractors of chaotic dynamical systems with fractal-fractional operators. Chaos Solitons Fractals 123:320-337

[17] Srivastava HM, Saad KM (2020) Numerical simulation of the fractal-fractional Ebola virus. Fractal Fract 4(4):49

[18] Atangana A (2017) Fractal-fractional differentiation and integration: Connecting fractal calculus and fractional calculus to predict complex system. Chaos Solitons Fractals 102:396−406 (2017)

[19] Wang W, Khan MA (2020) Analysis and numerical simulation of fractional model of bank data with fractal-fractional Atangana-Baleanu derivative. Journal of Computational and Applied Mathematics 369:112646

[20] Srivastava HM, Saad KM (2020) Numerical simulation of the fractal-fractional Ebola virus, Fractal Fract 4(4):1−13

[21] Rahimkhani P, Ordokhani Y, Sedaghat S (2023) The numerical treatment of fractal-fractional 2D optimal control problems by Müntz-Legendre polynomials. Optimal Control, Applications and Methods. https://doi.org/10.1002/oca.3024

[22] Heydari MH, Atangana A, Avazzadeh Z (2021) Numerical solution of nonlinear fractal-fractional optimal control problems by Legendre polynomials. Math Methods Appl Sci. 44(4):2952−2963

[23] Heydari MH, Atangana A, Avazzadeh Z, Yang Y (2020) Numerical treatment of the strongly coupled nonlinear fractal-fractional Schrödinger equations through the shifted Chebyshev cardinal functions. Math Meth Appl Sci 59(4):2037−2052

[24] Heydari MH, Avazzadeh Z, Atangana A (2021) Shifted Vieta-Fibonacci polynomials for the fractal-fractional fifth-order KdV equation. Math Meth Appl Sci 44:6716−6730.

[25] Srivastava HM, Saad KM, Hamanah WM (2022) Certain new models of the multi-space fractal-fractional Kuramoto-Sivashinsky and Korteweg-de Vries equations. Mathematics, Mathematics 10(7):1089.

[26] Alqhtani M, Saad KM (2022) Fractal-fractional Michaelis-Menten enzymatic reaction model via different kernels. Fractal and Fractional 6:13.

[27] Sabermahani S, Ordokhani Y, Rahimkhani P (2023) Application of generalized Lucas wavelet method for solving nonlinear fractal-fractional optimal control problems. Chaos, Solitons and Fractals 170:113348.

[28] Rahimkhani P, Heydari MH (2023) Fractional shifted Morgan-Voyce neural networks for solving fractal-fractional pantograph differential equations. Chaos, Solitons and Fractals 175:114070.

[29] Owolabi KM, Atangana A, Akgul A (2020) Modelling and analysis of fractal-fractional partial differential equations: application to reaction-diffusion model. Alex Eng J 1:1−17

[30] Zúñiga-Aguilar CJ, Gómez-Aguilar JF, Romero-Ugalde HM, Escobar-Jiménez RF, Fernández-Anaya G, Alsaadi FE (2022) Numerical solution of fractal-fractional Mittag-Leffler differential equations with variable-order using artificial neural networks. Engineering with Computers 38:pages 2669−2682

[31] Solís-Pérez JE, Gómez-Aguilar JF (2022) Variable-order fractal-fractional time delay equations with power, exponential and Mittag-Leffler laws and their numerical solutions. Engineering with Computers 38:555−577

[32] Rahimkhani P, Ordokhani Y, Sabermahani S (2023) Bernoulli wavelet least square support vector regression: Robust numerical method for a system of fractional differential equations. Mathematical Methods in the Applied Sciences. https://doi.org/10.1002/mma.9522

[33] Rahimkhani P, Ordokhani Y (2023) Hahn wavelets collocation method combined with Laplace transform method for solving fractional integro-differential equations. Mathematical Sciences. https://doi.org/10.1007/s40096-023-00514-3.

[34] Nemati S, Lima PM, Sedaghat S (2020) Legendre wavelet collocation method combined with the Gauss-Jacobi quadrature for solving fractional delay-type integro-differential equations. Appl Numer Math 149:99−112.

[35] Rahimkhani P, Ordokhani Y (2021) Numerical investigation of distributed-order fractional optimal control problems via Bernstein wavelets. Opt Control Appl Methods 42(1):355−373

[36] Keshavarz E, Ordokhani Y, Razzaghi M (2018) The Taylor wavelets method for solving the initial and boundary value problems of Bratu-type equations. Appl. Numer. Math. 128, 205−216

[37] Heydari MH (2020) Numerical solution of nonlinear 2D optimal control problems generated by Atangana-Riemann-Liouville fractal-fractional derivative. Applied Numerical Mathematics. 150, 507−518

[38] Rahimkhani P, Ordokhani Y (2020) Approximate solution of nonlinear fractional integro-differential equations using fractional alternative Legendre functions, Journal of Computational and Applied Mathematics 365:112365

[39] Do QH, Ngo HTB, Razzaghi M (2021) A generalized fractional-order Chebyshev wavelet method for two-dimensional distributed-order fractional differential equations. Communications in Nonlinear Science and Numerical Simulation 95:105597

[40] Sedaghat S, Mashayekhi S (2022) Exploiting delay differential equations solved by Eta functions as suitable mathematical tools for the investigation of thickness controlling in rolling mill. Chaos, Solitons and Fractals 164:112666

[41] Rahimkhani P, Ordokhani Y (2022) A modified numerical method based on Bernstein wavelets for numerical assessment of fractional variational and optimal control problems. Iranian Journal of Science and Technology, Transactions of Electrical Engineering, https://doi.org/10.1007/s40998-022-00522-4(0123456789().,-volV)(0123456789,-().volV)